Dalton Transactions

PAPER

View Article Online
View Journal | View Issue

Cite this: *Dalton Trans.*, 2015, **44**, 8506

A new class of luminescent Cu(I) complexes with tripodal ligands – TADF emitters for the yellow to red color range†

Timo Gneuß,[a] Markus J. Leitl,[b] Lars H. Finger,[a] Nicholas Rau,[a] Hartmut Yersin*[b] and Jörg Sundermeyer*[a]

Received 28th August 2014,
Accepted 10th November 2014

DOI: 10.1039/c4dt02631d

www.rsc.org/dalton

A new class of emissive and neutral Cu(I) compounds with tripodal ligands is presented. The complexes were characterized chemically, computationally, and photophysically. Under ambient conditions, the powders of the compounds exhibit yellow to red emission with quantum yields ranging from about 5% to 35%. The emission represents a thermally activated delayed fluorescence (TADF) combined with a short-lived phosphorescence which represents a rare situation and is a consequence of high spin–orbit coupling (SOC). In the series of the investigated compounds the non-radiative rates increase with decreasing emission energy according to the energy gap law while the radiative rate is almost constant. Furthermore, a well-fit linear dependence between the experimental emission energies and the transition energies calculated by DFT and TD-DFT methods could be established, thus supporting the applicability of these computational methods also to Cu(I) complexes.

Introduction

In the last few decades, luminescent copper(I) complexes have been intensely studied due to their structural and photophysical diversity.[1–12] Research in this field has gained additional momentum recently, since such complexes can be highly attractive for application in organic-light emitting diodes (OLEDs) or light-emitting electrochemical cells (LEECs).[13–27] This is because Cu(I) complexes often exhibit a thermally activated delayed fluorescence (TADF),[28–37] which allows utilizing all injected excitons for the generation of light by making use of the singlet harvesting effect.[28–32,34–37] In this regard, Cu(I) complexes can provide a low-cost alternative to expensive emitters based on 3rd row transition metals, such as platinum or iridium.[34,35,38–53]

For Cu(I) compounds, different structure motifs have been in the focus of research. In particular, extensive photophysical studies were conducted for copper(I) complexes that are pseudo-tetrahedrally coordinated by two bidentate chelating ligands. Homoleptic complexes with N^N (bisimine)[6,9,10,54–60] or P^P (bisphosphine)[54,61–63] ligands as well as heteroleptic complexes with N^N/P^P (bisimine/bisphosphine)[10,28,31,32,54,64–66] ligands were investigated. Typically, for such complexes optical or electrical excitation induces a metal-to-ligand charge transfer (MLCT) by which Cu(I) is formally oxidized to Cu(II).[1,5,6,9,31,32,56,67] Such a transition is accompanied by a flattening distortion towards a more planar geometry that promotes non-radiative deactivation pathways and as a consequence results in a reduction of the emission quantum yield.[2,10,28,31,32,57–59]

Also, several three-coordinate, trigonal Cu(I) complexes with one monodentate and one bidentate ligand have been studied.[20,37,68–73] These complexes exhibit structural reorganization on excitation as well, which is represented by the so-called Y→T shape distortion.[20,70,71] Similarly to the complexes with two bidentate ligands, these distortions result in an increased non-radiative deactivation.

Besides mononuclear complexes, dinuclear Cu(I) complexes and Cu(I) clusters have also been studied.[4,11,27,29,30,74–79]

In this work, a new class of luminescent mononuclear copper(I) halide complexes with tripodal ligands has been investigated. Compounds with this structural motif have been much less explored for their photophysical behavior. To our knowledge, only a few tripodally coordinated Cu(I) complexes have been investigated accordingly.[80,81] The complexes studied

[a]*Philipps-Universität Marburg, Materials Science Centre and Fachbereich Chemie, Hans-Meerwein-Straße 4, 35032 Marburg, Germany. E-mail: jsu@staff.uni-marburg.de; Fax: +49 (0)6421 28-25711; Tel: +49 (0)6421 28-25693*

[b]*Universität Regensburg, Institut für Physikalische Chemie, Universitätsstr. 31, 93053 Regensburg, Germany. E-mail: hartmut.yersin@ur.de; Fax: +49 (0)941 943-4488; Tel: +49 (0)941 943-4464*

†Electronic supplementary information (ESI) available: Discussion of the molecular structure of **tpyas**, packing diagrams of complexes **C1**, **C2** and **C3**, and details of quantum chemical calculations and emission spectra. CCDC 1021437–1021446. For ESI and crystallographic data in CIF or other electronic format see DOI: 10.1039/c4dt02631d

in this contribution are based on five different tripodal ligands, tris(2-pyridyl)phosphine oxide (tpypo) **L1**, tris(2-pyridyl)phosphine sulfide (tpyps) **L2**, tris(2-pyridyl)phosphine selenide (tpypse) **L3**, tris(2-pyridyl)arsine oxide (tpyaso) **L4**, and tris(2-pyridyl)methane (tpym) **L5**. By reacting these ligands with the respective copper halide CuX (X = Cl, Br, I), the complexes [CuCltpypo] **C1**, [CuBrtpypo] **C2**, [CuItpypo] **C3**, [CuCltpyps] **C4**, [CuBrtpyps] **C5**, [CuItpyps] **C6**, [CuItpypse] **C7**, [CuItpyaso] **C8**, and [CuItpym] **C9** were created. For these, the structures were determined using NMR spectroscopy, mass spectrometry, elemental analysis, and X-ray analysis. Moreover, photophysical studies and characterizations as well as quantum chemical calculations were carried out for this series of Cu(I) complexes.

Results and discussion

Synthesis of the ligands

The three ligands tpypo **L1**, tpyps **L2**, and tpypse **L3** were prepared in a two-step synthesis (Scheme 1). Tris(2-pyridyl)phosphine (tpyp) was synthesized from 2-bromopyridine and phosphorus trichloride *via* the classical method.[82,83] For this purpose 2-lithiopyridine was generated with *n*BuLi at −78 °C. Further reaction with phosphorus trichloride under salt elimination at −100 °C gave the desired product. Meanwhile, other synthetic methods are known to prepare tpyp, for example, with 2-bromopyridine and red phosphorus.[84–86] In the second step, the oxidized ligand tpypo **L1** was synthesized according to a previously published method, which was slightly modified. In the literature,[87–90] hydrogen peroxide solution was used to oxidize tpyp, whereas in our procedure *t*BuOOH (80% in DTBP) was used. The other two ligands tpyps **L2** and tpypse **L3** could be easily prepared by refluxing tpyp with elemental sulfur or gray selenium in toluene.[87,88] The progress of the reaction could be monitored *via* ^{31}P-NMR spectroscopy. An excess of sulfur or selenium in the reaction mixture was separated by filtration *via* a syringe filter. Yields between 45% and 94% were reached in the oxidation reactions.

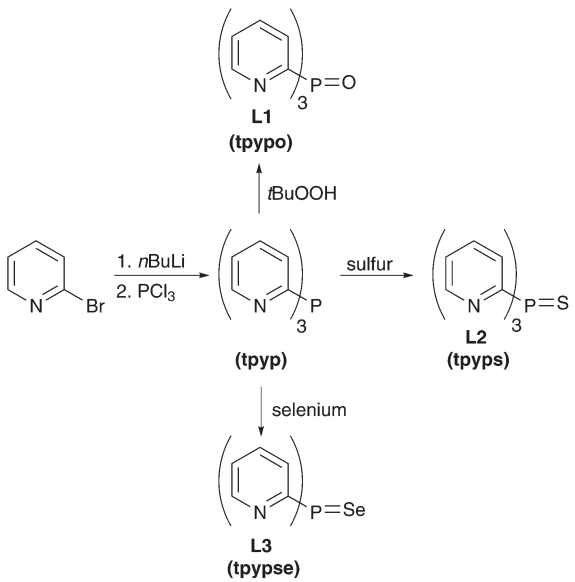

Scheme 1 Synthetic route to the ligands tpypo **L1**, tpyps **L2**, and tpypse **L3**.

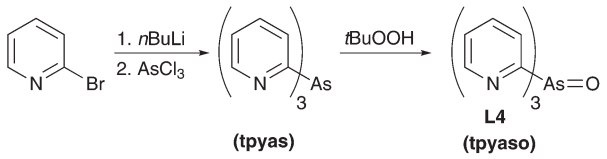

Scheme 2 Synthetic route to the arsine ligand tpyaso **L4**.

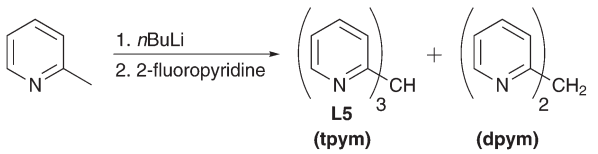

Scheme 3 Synthesis of the methane derivative tpym **L5**.

The synthesis of the arsine ligand tpyaso **L4** was carried out analogously to tpypo **L1**. First, the arsine compound tpyas is formed followed by oxidation with *t*BuOOH solution to tpyaso **L4** (Scheme 2). In contrast to tpyp, the arsine compound tpyas is stable in air.

The methane ligand tpym **L5** was prepared by a literature-known method.[91] First, 2-picoline is lithiated with *n*BuLi followed by reaction with 2-fluoropyridine under salt elimination (Scheme 3). The obtained mixture of the desired tpym **L5** and the by-product di(2-pyridyl)methane dpym was separated by distillation.

Synthesis of the copper(I) complexes

In this section the syntheses of nine new copper(I) complexes are presented (Scheme 4). To obtain the complexes, the ligand was dissolved in acetonitrile and reacted with a copper(I) halide (CuCl, CuBr, and CuI) at ambient temperature. A colored

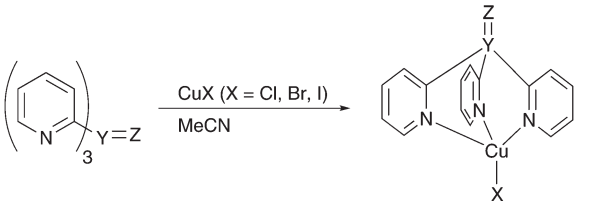

L1: Y = P, Z = O (**tpypo**)
L2: Y = P, Z = S (**tpyps**)
L3: Y = P, Z = Se (**tpypse**)
L4: Y = As, Z = O (**tpyaso**)
L5: Y = CH, Z = - (**tpym**)

C1: Y = P, Z = O, X = Cl **[CuCltpypo]**
C2: Y = P, Z = O, X = Br **[CuBrtpypo]**
C3: Y = P, Z = O, X = I **[CuItpypo]**
C4: Y = P, Z = S, X = Cl **[CuCltpyps]**
C5: Y = P, Z = S, X = Br **[CuBrtpyps]**
C6: Y = P, Z = S, X = I **[CuItpyps]**
C7: Y = P, Z = Se, X = I **[CuItpypse]**
C8: Y = As, Z = O, X = I **[CuItpyaso]**
C9: Y = CH, Z = -, X = I **[CuItpym]**

Scheme 4 Synthesized emissive copper(I) complexes.

precipitate was formed, which was collected by centrifugation. The yields of the different Cu(I) complexes varied significantly from 17% to 75%, depending on the solubility of the respective complex in the solvent.

We have also studied the coordination compounds of the phosphine tpyp with Cu(I) halide. Since the compounds are insoluble in common organic solvents, they could not be adequately characterized. It is assumed that the compounds are coordination polymers involving P–Cu interactions.

X-ray crystal structures

Crystal structures of tpyas and of the copper(I) complexes **C1–C9** have been determined using X-ray diffraction measurements. The crystallographic data and structure refinement details are summarized in Tables 1 and 2. Selected bond distances and angles are listed for ligand tpyas in Fig. S1† and for complexes **C1–C9** in Tables 3 and 4. The crystal structure of tpyas is discussed only in the ESI,† since no complexes have been made with this ligand.

Suitable single crystals of copper complexes **C1–C9** could be obtained from a saturated acetonitrile solution (at ambient temperature) after storing for a few days at 4 °C. The complexes crystallize either in the monoclinic or orthorhombic crystal system. As a representative example of all the copper compounds investigated here, the molecular structures of the three complexes [CuItpypo] **C3**, [CuItpyaso] **C8**, and [CuItpym] **C9** are shown in Fig. 1. The copper centers are coordinated by the halide anion and the three N atoms of the tripodal ligand in a distorted tetrahedral configuration. In each case, the halide atom deviates slightly from the Y–Cu axis (Y = P, As, C), which is due to packing effects that result from interactions with neighboring molecules (see Fig. S2–S4† for the three complexes **C1–C3** exhibiting the most pronounced bending of the halide). This is supported by quantum chemical calculations performed on the complex [CuCltpypo] **C1** which predict that the energy of the molecule is minimal if the chloride is lying on the P–Cu axis corresponding to an angle of P1–Cu1–Cl1 = 180°. However, bending the chloride away from this axis by 10°, corresponding to an angle of P1–Cu1–Cl1 = 170°, results only in a minor energy increase of 1 kJ mol^{-1}. This indicates that the potential energy surface describing the halide bending is very flat. For the three complexes [CuCltpypo] **C1**, [CuBrtpypo] **C2**, and [CuItpypo] **C3** the halide bending is most pronounced, with a bending angle of about 10° (P1–Cu1–X1 ≈ 170°) away from the P–Cu axis (see the angle Y(P, As, C)–Cu–X) in Tables 3 and 4). For the two complexes [CuBrtpyps] **C5** and [CuItpyps] **C6** with bonding angles of P1–Cu1–Br1 = 176.7(0)° and P1–Cu1–I1 = 178.4(1)°, respectively, the halide bending is relatively small.

The bond lengths of the various Cu–N bonds vary only slightly within the range of 2.027(3) Å to 2.091(2) Å for all investigated copper complexes. The bite angle N–Cu–N for the complexes with the tripodal phosphine ligands range from 93.2(4)° to 98.5(1)°. The bite angle is slightly larger for [Cultypaso] **C8** with the tripodal arsine ligand, with angles of N1–Cu1–N2 = 101.5(4)°, N1–Cu1–N3 = 97.3(4)°, and N2–Cu1–N3 = 97.4(4)°. In [CuItpym] **C9** with the tripodal methane ligand the bite angle is significantly smaller, with angles of N1–Cu1–N2 = 91.1(1)°, N1–Cu1–N3 = 89.7(1)°, and N2–Cu1–N3 = 90.7(1)°.

The Cu–X bond length increases from chloride to iodide due to the increasing atomic size of the halide, for example, in the series [CuXtpypo] from Cu1–Cl1 = 2.212(1) Å to Cu1–Br1 = 2.344(1) Å to Cu1–I1 = 2.499(1) Å. The bond length of the P–O bond is about 1.48 Å and that of the P–S bond is about 1.94 Å. Thereby they are in the range of the corresponding bond lengths of triphenylphosphine oxide (P–O 1.479(2) Å) and triphenylphosphine sulfide (P–S 1.950(3) Å).[92,93]

Computational studies

To learn more about the tripodally coordinated copper complexes, quantum chemical calculations have been carried out for complexes **C1–C3** and **C6–C9**, using density functional theory (DFT) and time-dependent density functional theory (TD-DFT) with the functional B3LYP and the basis set def2-TZVPP. It has been shown that this method gives good results for Cu(I) complexes, especially for a description of the transition energies.[94]

We want to focus the discussion on [CuItpypo] **C3**. For this compound, the optimized ground state geometry and the first excited triplet state geometry were calculated. The results are displayed in Fig. 2. In the ground state, the halide is lying on the axis that is defined by the P1–Cu1 atoms (Fig. 2a). However, in the triplet state geometry, the halide is bent away from this axis (Fig. 2b). This is clearly displayed by the three I–Cu–N angles. In the ground state geometry, all three angles I–Cu–N are nearly equivalent to values of about 123°. In the triplet state, the angle I1–Cu1–N1, amounting to 110.3°, is significantly smaller while the two other angles, I1–Cu1–N2 amounting to 127.4° and I1–Cu1–N3 amounting to 128.3°, are slightly larger than in the ground state (compare with Table S1†). Moreover, it can be seen that in the triplet state geometry two Cu–N bonds are distinctly shortened, *i.e.* from the ground state value of 2.145 Å to 1.986 Å (Cu1–N2) and from 2.144 Å to 1.985 Å (Cu1–N3), respectively, while the Cu1–N1 bond length increases from 2.146 Å to 2.265 Å. This shows that two Cu–N bonds are strengthened and one Cu–N bond is weakened in the triplet state.

The occurrence of such a distortion in the excited state can be understood when the composition of the frontier orbitals is analyzed (Fig. 3). For [CuItpypo] **C3**, the HOMO is mainly localized on the copper atom and the halide, whereas the LUMO is mainly distributed over two of the three pyridine moieties of the tripod ligand. TD-DFT calculations reveal that transitions between these frontier orbitals largely determine the first excited singlet state S_1 and triplet state T_1, especially in the triplet state geometry. Therefore, these states can be classified to be of (metal + halide)-to-ligand charge transfer (^{1,3}(M + X) LCT) character. To quantify the amount of charge that is transferred on excitation the *natural charges* for the copper and iodine atoms were calculated for the ground and the first excited triplet state. They amount to +0.321 (Cu) and −0.562 (I)

Table 1 Crystallographic data for tpyas and **C1–C4**

	tpyas	C1	C2	C3	C4
Habitus	Block	Needle	Needle	Needle	Needle
Color	Colourless	Red	Orange	Red	Red
Formula	$C_{15}H_{12}AsN_3$	$C_{16}H_{13.50}ClCuN_{3.50}OP$	$C_{16.50}H_{14.25}BrCuN_{3.75}OP$	$C_{16.50}H_{14.25}CuIN_{3.75}OP$	$C_{18}H_{16.50}ClCuN_{4.50}PS$
Fw [g mol^{-1}]	309.20	400.76	455.49	502.48	457.88
Crystal size [mm]	0.230 × 0.230 × 0.220	0.660 × 0.260 × 0.190	0.450 × 0.190 × 0.130	0.210 × 0.040 × 0.040	0.250 × 0.040 × 0.040
Crystal system	Monoclinic	Orthorhombic	Monoclinic	Monoclinic	Orthorhombic
Space group	*P*21/*c*	*Pbca*	*P*21/*n*	*P*21/*n*	*Pccn*
a [Å]	9.1529(9)	8.4558(6)	8.5684(10)	8.6959(3)	15.0776(12)
b [Å]	9.1102(6)	27.6843(13)	28.964(3)	29.6332(11)	30.280(2)
c [Å]	16.0342(16)	28.3435(16)	14.501(2)	14.5579(6)	8.6832(4)
α [°]	90	90	90	90	90
β [°]	100.982(8)	90	106.175(5)	105.894(3)	90
γ [°]	90	90	90	90	90
Cell volume [Å^3]	1312.5(2)	6635.0(7)	3456.3(7)	3608.0(2)	3964.3(4)
Z	4	16	8	8	8
D_{calc} [Mg m^{-3}]	1.565	1.605	1.751	1.850	1.534
Abs. coeff. [mm^{-1}]	2.578	1.582	3.679	3.021	1.434
F(000)	624	3248	1812	1956	1864
T [K]	100(2)	100(2)	100(2)	100(2)	100(2)
λ [Å]	0.71073	0.71069	0.71069	0.71069	0.71069
Reflns collected	8036	25 305	21 656	33 130	13 790
Indep. reflns	2763	7307	7647	7632	4187
Obs. reflns [$I > 2(I)$]	2318	5432	4427	4265	1823
Reflns used for refin.	2763	7307	7647	7632	4187
Abs. Correction	Semi-empirical	Semi-empirical	Semi-empirical	Analytical	Semi-empirical
GOF	0.964	1.037	1.031	0.689	0.715
wR_2	0.0666	0.1677	0.1068	0.0492	0.0703
R_1 [$I > 2\sigma(I)$]	0.0254	0.0658	0.0610	0.0300	0.0417

Table 2 Crystallographic data for **C5–C9**

	C5	C6	C7	C8	C9
Habitus	Plate	Block	Needle	Needle	Plate
Color	Orange	Orange	Orange	Yellow	Yellow
Formula	$C_{20}H_{19.50}BrCuN_{5.50}PS$	$C_{47}H_{39}Cu_3I_3N_{10}P_3S_3$	$C_{20}H_{19.50}CuIN_{5.50}PSe$	$C_{16.50}H_{14.25}AsCuIN_{3.75}O$	$C_{16}H_{13}CuIN_3$
Fw[g mol^{-1}]	543.39	1504.35	637.28	546.43	437.73
Crystal size [mm]	0.200 × 0.130 × 0.050	0.310 × 0.280 × 0.180	0.440 × 0.110 × 0.040	0.280 × 0.050 × 0.040	0.490 × 0.250 × 0.100
Crystal system	Monoclinic	Orthorhombic	Monoclinic	Monoclinic	Monoclinic
Space group	*P*21/*a*	*Pc*21*b*	*P*21/*a*	*P*21/*n*	*P*21/*n*
a [Å]	8.5838(3)	13.2413(5)	8.7685(3)	8.7081(4)	14.7528(4)
b [Å]	15.2046(7)	15.7217(6)	15.6075(5)	29.7666(14)	13.4193(3)
c [Å]	17.8716(6)	25.7987(11)	18.0144(8)	14.5936(9)	16.0010(4)
α [°]	90	90	90	90	90
β [°]	103.386(3)	90	104.011(3)	105.559(4)	90.266(2)
γ [°]	90	90	90	90	90
Cell volume [Å^3]	2269.11(15)	5370.7(4)	2392.00(16)	3644.2(3)	3167.72(14)
Z	4	4	4	8	8
D_{calc} [Mg m^{-3}]	1.591	1.860	1.770	1.992	1.836
Abs. coeff. [mm^{-1}]	2.904	3.152	3.809	4.705	3.324
F(000)	1092	2920	1236	2100	1696
T [K]	100(2)	100(2)	100(2)	100(2)	100(2)
λ [Å]	0.71069	0.71069	0.71069	0.71069	0.71069
Reflns collected	17 036	18 930	13 242	35 607	47 871
Indep. reflns	4804	10 265	5056	35 607	6720
Obs. reflns [$I > 2(I)$]	3562	6869	3816	16 911	5801
Reflns used for refin.	4804	10 265	5056	35 607	6720
Abs. correction	Semi-empirical	Semi-empirical	Semi-empirical	Integration	Semi-empirical
GOF	1.085	0.747	0.865	0.764	1.098
wR_2	0.1196	0.0822	0.0613	0.1465	0.0745
R_1 [$I > 2\sigma(I)$]	0.0522	0.0376	0.0298	0.0580	0.0274

for the ground state (S_0 geometry) and to +0.665 (Cu) and −0.324 (I) for the first excited triplet state (T_1 geometry). This nicely confirms the occurrence of a pronounced charge transfer away from the metal and halide upon excitation. Especially, the transfer of charge away from the copper center, in a rather crude approximation representing a formal oxidation of Cu(I)

Table 3 Selected bond distances [Å] and angles [°] for **C1–C5**

C1	C2	C3	C4	C5
Cu1–N1 2.067(3)	Cu1–N1 2.072(4)	Cu1–N1 2.062(3)	Cu1–N1 2.078(3)	Cu1–N1 2.043(4)
Cu1–N2 2.047(4)	Cu1–N2 2.063(5)	Cu1–N2 2.060(3)	Cu1–N2 2.063(3)	Cu1–N2 2.052(4)
Cu1–N3 2.047(3)	Cu1–N3 2.049(5)	Cu1–N3 2.049(4)	Cu1–N3 2.027(3)	Cu1–N3 2.048(4)
Cu1–Cl1 2.212(1)	Cu1–Br1 2.344(1)	Cu1–I1 2.499(1)	Cu1–Cl1 2.230(1)	Cu1–Br1 2.335(1)
P1–O1 1.489(3)	P1–O1 1.479(4)	P1–O1 1.477(3)	P1–S1 1.942(2)	P1–S1 1.944(2)
P1–C1 1.828(4)	P1–C1 1.830(6)	P1–C1 1.820(4)	P1–C1 1.837(4)	P1–C1 1.835(5)
P1–C6 1.820(4)	P1–C6 1.812(6)	P1–C6 1.829(4)	P1–C6 1.827(4)	P1–C6 1.827(5)
P1–C11 1.827(4)	P1–C11 1.818(6)	P1–C11 1.820(5)	P1–C11 1.817(4)	P1–C11 1.825(5)
Cl1–Cu1–N1 113.8(1)	Br1–Cu1–N1 111.9(1)	I1–Cu1–N1 112.6(1)	Cl1–Cu1–N1 114.9(1)	Br1–Cu1–N1 121.7(1)
Cl1–Cu1–N2 116.8(1)	Br1–Cu1–N2 118.7(1)	I1–Cu1–N2 119.7(1)	Cl1–Cu1–N2 117.5(1)	Br1–Cu1–N2 122.6(1)
Cl1–Cu1–N3 131.1(1)	Br1–Cu1–N3 131.5(1)	I1–Cu1–N3 129.7(1)	Cl1–Cu1–N3 129.6(1)	Br1–Cu1–N3 117.8(1)
N1–Cu1–N2 97.3(1)	N1–Cu1–N2 98.3(2)	N1–Cu1–N2 98.5(1)	N1–Cu1–N2 95.1(1)	N1–Cu1–N2 95.8(2)
N1–Cu1–N3 95.3(1)	N1–Cu1–N3 95.9(2)	N1–Cu1–N3 95.6(1)	N1–Cu1–N3 96.7(1)	N1–Cu1–N3 96.4(2)
N2–Cu1–N3 96.1(1)	N2–Cu1–N3 94.1(2)	N2–Cu1–N3 94.5(1)	N2–Cu1–N3 96.1(2)	N2–Cu1–N3 96.5(2)
O1–P1–C1 113.2(2)	O1–P1–C1 113.8(2)	O1–P1–C1 113.6(2)	S1–P1–C1 113.5(2)	S1–P1–C1 113.3(2)
O1–P1–C6 113.4(2)	O1–P1–C6 113.2(3)	O1–P1–C6 112.6(2)	S1–P1–C6 114.0(1)	S1–P1–C6 113.8(2)
O1–P1–C11 112.9(2)	O1–P1–C11 113.0(3)	O1–P1–C11 113.3(2)	S1–P1–C11 112.5(2)	S1–P1–C11 113.5(2)
P1–Cu1–Cl1 168.9(0)	P1–Cu1–Br1 168.1(1)	P1–Cu1–I1 169.8(0)	P1–Cu1–Cl1 170.5(0)	P1–Cu1–Br1 176.7(0)

Table 4 Selected bond distances [Å] and angles [°] for **C6–C9**

C6	C7	C8	C9
Cu1–N1 2.069(9)	Cu1–N1 2.054(3)	Cu1–N1 2.058(9)	Cu1–N1 2.091(2)
Cu1–N2 2.068(10)	Cu1–N2 2.043(3)	Cu1–N2 2.063(10)	Cu1–N2 2.074(2)
Cu1–N3 2.056(9)	Cu1–N3 2.046(3)	Cu1–N3 2.055(10)	Cu1–N3 2.057(2)
Cu1–I1 2.512(1)	Cu1–I1 2.486(1)	Cu1–I1 2.510(2)	Cu1–I1 2.465(0)
P1–S1 1.935(3)	P1–Se1 2.104(1)	As1–O1 1.636(8)	
P1–C1 1.846(12)	P1–C1 1.840(4)	As1–C1 1.936(12)	C16–C1 1.523(3)
P1–C6 1.816(12)	P1–C6 1.843(4)	As1–C6 1.935(12)	C16–C6 1.524(3)
P1–C11 1.841(11)	P1–C11 1.838(4)	As1–C11 1.936(13)	C16–C11 1.524(3)
I1–Cu1–N1 119.9(3)	I1–Cu1–N1 117.8(1)	I1–Cu1–N1 111.1(3)	I1–Cu1–N1 117.9(1)
I1–Cu1–N2 122.5(3)	I1–Cu1–N2 120.0(1)	I1–Cu1–N2 118.4(3)	I1–Cu1–N2 126.8(1)
I1–Cu1–N3 122.6(3)	I1–Cu1–N3 124.2(1)	I1–Cu1–N3 126.6(3)	I1–Cu1–N3 129.5(1)
N1–Cu1–N2 93.2(4)	N1–Cu1–N2 96.4(1)	N1–Cu1–N2 101.5(4)	N1–Cu1–N2 91.1(1)
N1–Cu1–N3 96.9(4)	N1–Cu1–N3 96.2(1)	N1–Cu1–N3 97.3(4)	N1–Cu1–N3 89.7(1)
N2–Cu1–N3 94.8(4)	N2–Cu1–N3 96.3(1)	N2–Cu1–N3 97.4(4)	N2–Cu1–N3 90.7(1)
S1–P1–C1 113.4(4)	Se1–P1–C1 113.1(1)	O1–As1–C1 114.1(5)	H16–C16–C1 107.1
S1–P1–C6 113.9(4)	Se1–P1–C6 112.9(1)	O1–As1–C6 112.6(5)	H16–C16–C6 107.1
S1–P1–C11 113.5(4)	Se1–P1–C11 114.2(1)	O1–As1–C11 114.2(5)	H16–C16–C11 107.1
P1–Cu1–I1 178.4(1)	P1–Cu1–I1 176.0(0)	As1–Cu1–I1 170.6(1)	C16–Cu1–I1 172.7(0)

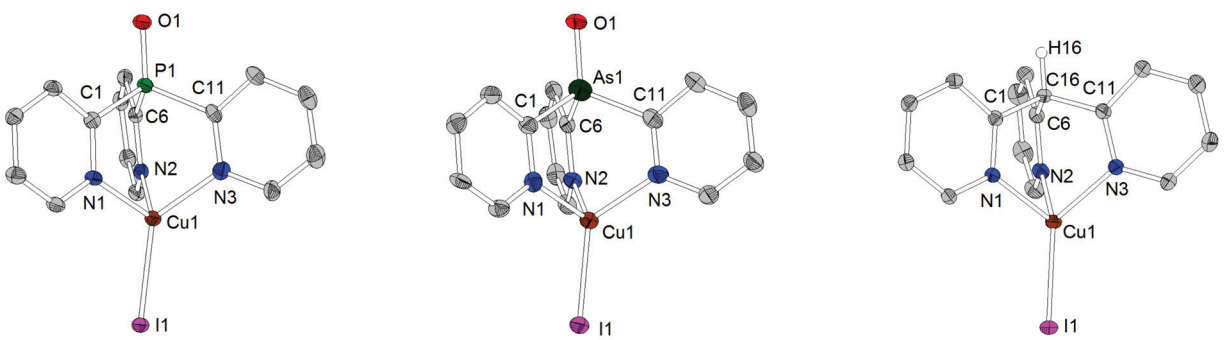

[Cultpypo] **C3** [Cultpyaso] **C8** [Cultpym] **C9**

Fig. 1 Molecular structures of [Cultpypo] **C3**, [Cultpyaso] **C8**, and [Cultpym] **C9** (thermal ellipsoids with 50% probability) resulting from X-ray analyses. Hydrogen atoms (except for H16 of **C9**) and solvent molecules are omitted for clarity.

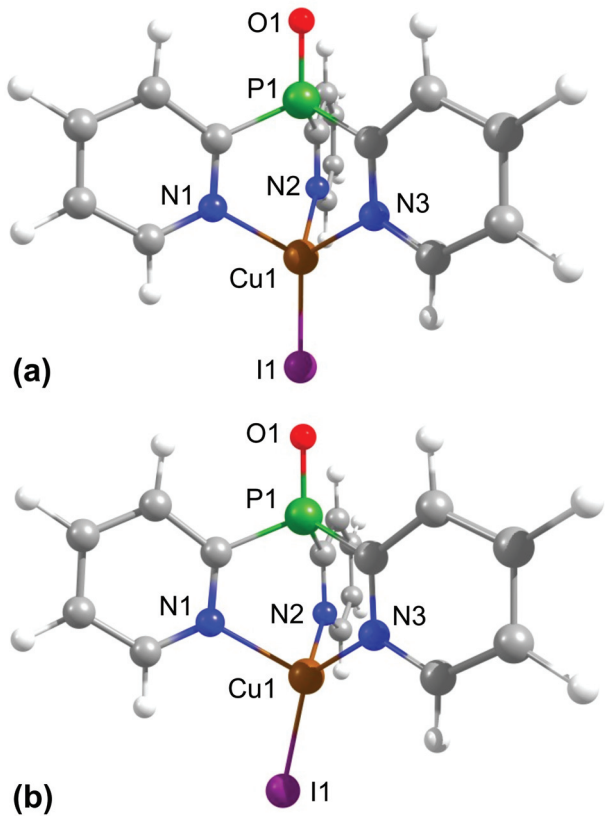

Fig. 2 Optimized ground state (a) and first excited triplet state (b) geometries of [CuItpypo] **C3**. Calculations were performed on the B3LYP/def2-TZVPP level of theory.

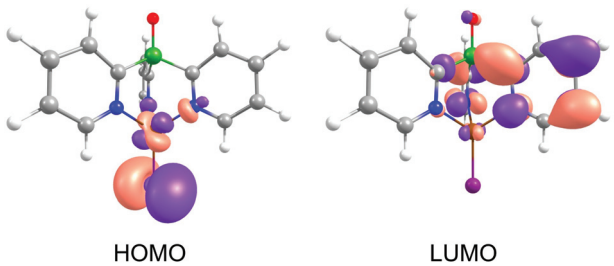

Fig. 3 Contour surfaces of HOMO and LUMO for [CuItpypo] **C3** calculated for the ground state geometry. Calculations were performed on the B3LYP/def2-TZVPP level of theory. The contour value of the MOs amounts to 0.04.

to Cu(II), has an important consequence. As Cu(I) prefers a tetrahedral coordination environment, whereas Cu(II) prefers a planar one, significant structural reorganizations occur upon excitation. In the case of [CuItpypo] **C3** these reorganizations are mainly represented by the bending of the halide away from the Cu–P axis and by changes of the Cu–N binding distances as described above.

Interestingly, a comparison of the two tripodal copper complexes, K[Cu(SC_6F_5)(HB(3,5-^{i}Pr$_2$pz)$_3$)], representing a Cu(I) complex, and [Cu(SC_6F_5)(HB(3,5-^{i}Pr$_2$pz)$_3$)], representing a Cu(II) complex, supports the results that are predicted from our calculations.[95,96] Compared to the Cu(I) complex, two of the three Cu–N bonds are shorter for the Cu(II) homologue (Cu(I): Cu–N11 = 2.188(7) Å, Cu–N31 = 2.062(7) Å; Cu(II): Cu–N11 = 2.037(9) Å, Cu–N31 = 1.930(9) Å), whereas the third Cu–N bond is longer (Cu(I): Cu–N21 = 2.065(7) Å; Cu(II): Cu–N21 = 2.119(8) Å). Moreover, the bending of the thiolate away from the B–Cu axis is by about 7° larger for the Cu(II) complex than for the Cu(I) homologue (Cu(I): B–Cu–S = 174°, Cu(II): B–Cu–S = 167°).

For completeness it is remarked that similar geometry distortions for the triplet state geometry were also found for all other complexes presented in this study. This is shown in Table S1† also for the two complexes [CuItpyaso] **C8** and [CuItpym] **C9**.

In the scope of our calculations, the energy gaps between HOMO and LUMO show only slight variations between about 2.5 and 2.7 eV (data for all complexes are summarized in Table S2†). For an estimate of the transition energies, a comparison of the HOMO–LUMO gaps is, however, not sufficient. Instead, TD-DFT calculations have been performed.

The TD-DFT transition energies of the different compounds, as calculated for the optimized T_1 state geometry, differ significantly from the experimental emission energies (see Table S3†). However, it is not expected that these calculated gas phase data can exactly reproduce the experimental data, since (i) TD-DFT results have the tendency to underestimate the transition energies that correspond to charge-transfer states[94,97,98] and since (ii) especially for Cu(I) complexes, the experimental emission energies depend strongly on the environment and, in particular, on its rigidity,[28,31,32] which is not taken into account in our calculations. Nevertheless, the calculated transition energies nicely reproduce the trend of the emission energies as determined for the Cu(I) complexes doped into amorphous PMMA (polymethylmethacrylate) (Fig. 4). It is remarked that the experimental trend is not repro-

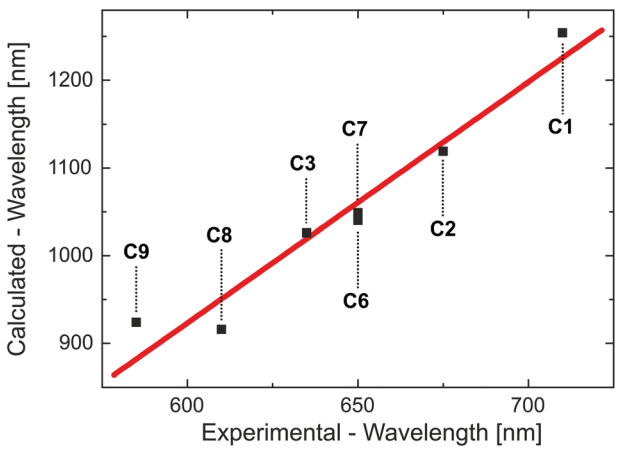

Fig. 4 Calculated $T_1 \rightarrow S_0$ transition wavelength *versus* experimentally determined emission wavelengths for different Cu(I) complexes as defined in Scheme 4. The calculated values result from TD-DFT calculations performed for the optimized triplet state geometry. The experimental values represent the emission maxima as found for compounds doped into PMMA. The red line represents a linear fit to the data points. The coefficient of determination for this fit amounts to R^2 = 0.92.

duced by TD-DFT calculations performed for the ground state geometry.

Furthermore, our calculations suggest that the energy separations $\Delta E(S_1–T_1)$ between the T_1 and S_1 states are rather small, lying between about 1000 and 1350 cm^{-1} (compare Table S3†). For such small energy splittings the occurrence of a thermally activated delayed fluorescence is expected. A more detailed discussion of this aspect is presented in the next section.

Photophysical studies

Again, the discussion will focus on [CuItpypo] **C3**. Fig. 5 shows the absorption spectrum of this compound *and* of the tpypo **L1** ligand recorded in dichloromethane. The absorption bands observed in the range between about 230 nm and 300 nm are present in both the complex and the ligand. Therefore, they are assigned to result from ligand centered transitions. In contrast, in the range between about 300 and 500 nm, the ligand does not absorb, but for the complex two separate absorption bands are observed. This allows us to assign these bands to charge transfer transitions in agreement with the results obtained from DFT and TD-DFT calculations that predict low-lying (M + X)LCT states.

In fluid solution, an emission of [CuItpypo] **C3** is not observed at ambient temperature even after oxygen was carefully removed by at least five freeze–pump–thaw cycles. In contrast, when doped into a PMMA matrix, the complex exhibits a red emission with a maximum at λ_{max} = 635 nm and an emission quantum yield of Φ_{PL} = 16%. As powder, the emission is orange with a maximum at λ_{max} = 600 nm and a quantum yield of Φ_{PL} = 20% (Fig. 5).

The emission of [CuItpypo] **C3** in PMMA compared to the neat powder is red shifted by 35 nm. This can be attributed to differences in matrix rigidity. With decreasing rigidity the complex can undergo more distinct distortions upon (M + X) LCT excitation resulting in an energy stabilization of the emitting state(s). In addition to this red shift, the distortions cause an increase of non-radiative deactivations to the ground state due to increased Franck Condon factors that couple the excited state to the ground state.[99,100] As a consequence, the quantum yield decreases with decreasing rigidity of the environment from 20% (powder) to 16% (PMMA) to ≪1% (solution).

The emission decay time and its temperature dependence show further important information. As for [CuItpypo] **C3** doped into PMMA the decay strongly deviates from a mono-exponential behavior (due to distinct inhomogeneity effects),[101] we focus on the emission properties of the powders.[102] At ambient temperature, an emission decay time of τ(300 K) = 4 μs and an emission quantum yield of Φ_{PL}(300 K) = 20% are found for [CuItpypo] **C3**. When the powder sample is cooled to T = 77 K, the decay time increases to τ(77 K) = 24 μs and the emission quantum yield to Φ_{PL}(77 K) = 63%. Calculation of the radiative and non-radiative rates according to $k_r = \Phi_{PL}\tau^{-1}$ and $k_{nr} = (1 - \Phi_{PL})\tau^{-1}$, respectively, reveals that the radiative rate increases by a factor of about two from k_r(77 K) = 3 × 10^4 s^{-1} to k_r(300 K) = 5 × 10^4 s^{-1}, whereas the non-radiative rate increases tenfold from k_{nr}(77 K) = 2 × 10^4 s^{-1} to k_{nr}(300 K) = 2 × 10^5 s^{-1}. Furthermore, the powder sample shows a slight blue-shift of the emission maximum from λ_{max}(77 K) = 610 nm to λ_{max}(300 K) = 600 nm.

An increase of the radiative rate and a blue-shift of the emission on increasing the temperature from T = 77 K to 300 K has often been reported for Cu(I) complexes and can be explained by the occurrence of a thermally activated delayed fluorescence (TADF).[28–32,34,35] Accordingly, at low temperature, only emission from the lowest excited triplet state T_1 occurs. With temperature increase, a thermal population of the energetically only slightly higher lying first excited singlet state S_1 becomes possible. As the $S_1 \rightarrow S_0$ transition is significantly more allowed than the spin-forbidden $T_1 \rightarrow S_0$ transition, an effective reduction of the emission decay time results. Moreover, as the S_1 state lies energetically higher than the T_1 state, a blue shift of the emission is expected to occur with increasing temperature.

However, for the compound [CuItpypo] **C3**, only a moderate increase of the radiative rate by a factor of about 2 was found to occur on heating. This is much less than what has been reported for other Cu(I) complexes. For example, the compounds presented in ref. 29 (Cu(I) halide dimers with different chelating aminophosphane ligands) experience a radiative rate increase by a factor of 40 to 150 and the compound discussed in ref. 36 (Cu(I) chloride dimer with a chelating diphosphane ligand) even shows a much higher factor of 490. The small radiative rate increase found for [CuItpypo] **C3** can be rationalized by taking into account an additional and efficient emission decay path from the triplet state to the singlet ground state. The compounds discussed in ref. 29 and 36 exhibit long triplet decay times between 250 μs and 2200 μs. In contrast, the triplet decay time of [CuItpypo] **C3** amounts to only 24 μs

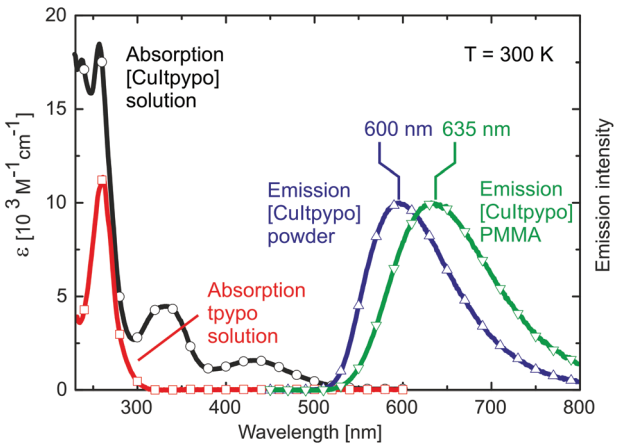

Fig. 5 Absorption spectra of the ligand tpypo **L1** and the corresponding complex [CuItpypo] **C3** recorded in a dichloromethane solution. Emission spectra are displayed for [CuItpypo] **C3** as a powder and doped into a PMMA matrix, respectively. All measurements were recorded under ambient conditions.

(T = 77 K value). As a consequence, a further shortening of the emission decay time by involving the TADF mechanism at higher temperature is much less effective. Further support for this interpretation is given in ref. 37 (three-coordinate Cu(I) carbene complex) where a Cu(I) complex with a similarly short triplet decay time of 34 μs is investigated. This compound also displays only a moderate increase of the radiative rate by a factor of about 3 when the TADF process is activated.

Obviously, the only moderate increase of the radiative rate upon heating can be rationalized by a significant contribution of the triplet state emission even at ambient temperature. Accordingly, both the singlet state S_1 and the triplet state T_1 contribute to the overall emission at ambient temperature. Consequently, the expected blue-shift of the emission maximum with increasing temperature is not as clearly displayed for the studied complexes as for TADF-only emitters (compare ref. 28–32, 34–36). However, the corresponding blue-shift is displayed on the high-energy flanks of the spectra measured at T = 77 K and 300 K, respectively (compare with Table 5).

Fig. 6 shows the emission spectra of the compounds **C1–C3** and **C6–C9**. The complexes [CuCltpypo] **C1** and [CuBrtpypo] **C2** exhibit the same trends in the emission behavior as those described for [CuItpypo] **C3**. For all the other investigated compounds corresponding trends are expected to occur. An overview of the respective emission parameters is given in Table 5. The complexes [CuCltpyps] **C4** and [CuBrtpyps] **C5** exhibit very similar emission properties to complexes [CuCltpypo] **C1** and [CuBrtpypo] **C2**, respectively. Therefore, these are not explicitly discussed here.

Table 5 Emission properties of compounds **C1–C3** and **C6–C9** as powders at T = 77 K and 300 K. λ_{max} represents the wavelength at the maximum of the emission spectrum and $\lambda_{50\%}$ the wavelength at 50% of the maximum at the high energy flank of the spectrum

	Temp. [K]	λ_{max} [nm]	$\lambda_{50\%}$ [nm]	τ [μs]	Φ_{PL} [%]	k_r [10^4 s^{-1}]	k_{nr} [10^4 s^{-1}]
[CuCltpypo] **C1**	300	645	595	3	8	3	30
	77	645	610	13	14	1	7
[CuBrtpypo] **C2**	300	620	575	4	18	5	20
	77	620	585	20	36	2	3
[CuItpypo] **C3**	300	600	550	4	20	5	20
	77	610	555	24	63	3	2
[CuItpyps] **C6**	300	595	555	8	34	4	8
	77	595	565	24			
[CuItpypse] **C7**	300	640	595	2	4	2	50
	77	675	630	9			
[CuItpyaso] **C8**	300	600	550	4	12	3	20
	77	610	565	23			
[CuItpym] **C9**	300	550	510	5	28	6	10
	77	550	530	22			

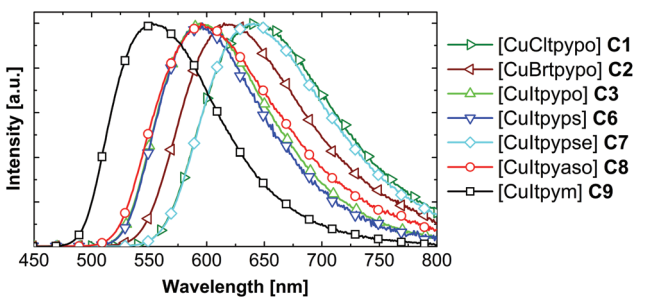

Fig. 6 Emission spectra of the investigated complexes as powders at ambient temperature. The samples were excited at λ_{exc} = 350 nm.

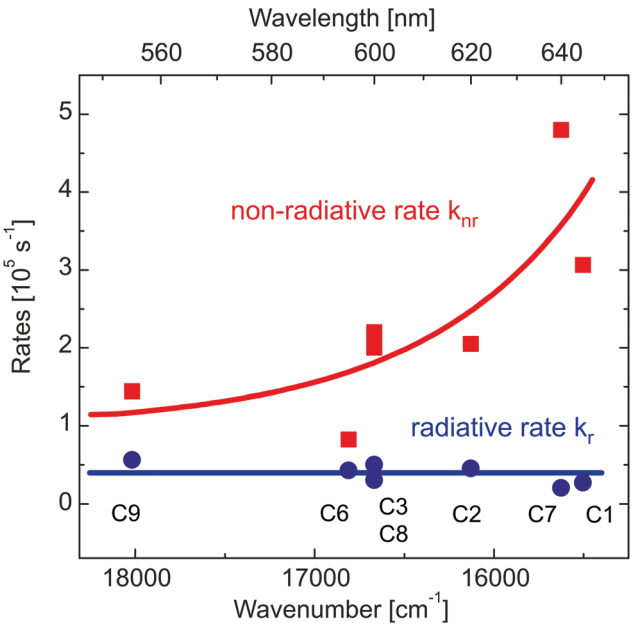

Fig. 7 Radiative k_r and non-radiative rates k_{nr} of the investigated compounds *versus* emission energy. Data are given for the powders of the complexes at ambient temperature. The curves are displayed as a guide for the eye.

An analysis of the radiative and non-radiative rates for the studied series of complexes reveals an interesting trend. At ambient temperature, powders of all compounds show similar radiative rates k_r ranging from 3×10^4 to 6×10^4 s^{-1}. In contrast, the non-radiative rates k_{nr} increase drastically with increasing emission wavelength. Such a trend is not unexpected and can be described by the energy gap law. In its simplest form it can be written as[103]

$$k_{nr} \sim \exp[-\gamma \Delta E/(\hbar \omega_n)] \quad (1)$$

wherein ΔE represents the energy separation between the states involved in the transition, γ a molecular coupling parameter, $\hbar$ the Planck constant, and ω_n the dominant vibrational frequency that induces the non-radiative process. Accordingly, an exponential dependence of the non-radiative rate k_{nr} on the emission energy ΔE is expected to occur. Indeed, this is experimentally observed. A graphical representation of this correlation is given in Fig. 7. These results demonstrate that the realization of compounds showing efficient red light emission remains a challenging task.

Conclusion and outlook

Emitter materials that exhibit a thermally activated delayed fluorescence (TADF) or a phosphorescence are highly attractive for use in OLEDs as they can convert all injected excitons into light. For applications, the emitter should also exhibit a short (radiative) decay time to minimize saturation effects.[104] The complexes investigated in this study are interesting in this regard; when compared to other Cu(I) complexes they exhibit relatively short phosphorescence ($T_1 \rightarrow S_0$ emission) decay times, for example, amounting to only about 24 μs (radiative decay time 38 μs) in the case of [CuItpypo] **C3**. Thus, it can be concluded that spin–orbit coupling is particularly effective when compared to other Cu(I) complexes for which triplet decay times of several hundred microseconds or longer are not unusual.[29,32,36] Besides this already effective radiative deactivation process *via* phosphorescence, an additional radiative TADF path becomes important at ambient temperature for the investigated compounds. The combined emission paths of phosphorescence and TADF result in a distinct increase of the overall radiative rate when compared to TADF-only emitters. This property is highly attractive when the compounds are applied as emitters in OLEDs, in particular, to reduce saturation effects.

Another interesting observation was made for the investigated compounds. In this series, the non-radiative rate increases strongly with decreasing emission energy following the energy gap law. As a consequence, the emission quantum yields decrease towards the red range of the spectrum from 28% for [CuItpym] **C3** to 4% for [CuItpypse] **C7**. Accordingly, shifting the emission to the blue using methods of chemical engineering will result in a significant reduction of the non-radiative rates and will therefore lead to an increase of the emission quantum yield. An extrapolation of the data presented to shorter wavelengths reveals that for an emission wavelength of 460 nm, an emission quantum yield greater than 70% would be expected.

Experimental

General remarks

The syntheses and handling of air- and moisture-sensitive substances were carried out using standard Schlenk and glovebox techniques. Solvents were dried using standard procedures[105] and stored over Al_2O_3/molecular sieves 3 Å/R3-11G catalyst (BASF).

The starting materials were obtained from commercial sources (Sigma-Aldrich, Merck, Acros Organics, Alfa Aesar) and used as received. The following materials were prepared according to literature procedures: tris(2-pyridyl)phosphine[82,83] (tpyp), tris(2-pyridyl)methane[91] (tpym) **L5**, copper(I) chloride[106], and copper(I) iodide.[107]

NMR spectra were recorded at 300 K on a Bruker DPX 250, Bruker ARX 300, Bruker DRX 400, Bruker ARX 500, or Bruker DRX 500 using $CDCl_3$ or DMSO-d_6 as the solvent. Chemical shifts are given with respect to tetramethylsilane (^{1}H, ^{13}C) and phosphoric acid (^{31}P). Calibration of ^{1}H and ^{13}C NMR spectra was accomplished with the solvent signals, and ^{31}P spectra were calibrated externally.

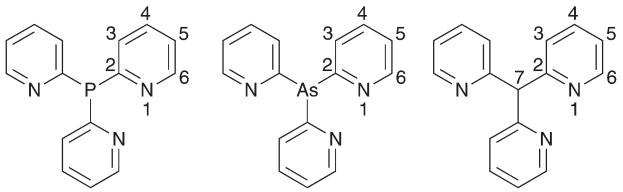

Fig. 8 Example of the numbering of compounds.

The numbering of the hydrogen and carbon atoms is shown for the three ligands tpyp, tpyas, and tpym in Fig. 8.

Electrospray ionization (ESI) mass spectra were recorded on a Thermo Fisher Scientific LTQ FT Ultra using methanol, acetonitrile, or dichloromethane as the solvent. IR spectra were recorded on a Bruker Alpha FT-IR spectrometer using powder samples at ambient temperature. Elemental analysis was done using an Elementar vario MICRO cube. UV-Vis absorption measurements were carried out using a Varian Cary 300 double beam spectrometer. Emission spectra were recorded with a Fluorolog 3-22 (Horiba Jobin Yvon) spectrophotometer which was equipped with a cooled photo-multiplier (RCA C7164R). For the decay time measurements, the same photomultiplier was used in combination with a FAST ComTec multichannel scaler PCI card with a time resolution of 250 ps. As the excitation source for the decay time measurements, a pulsed diode laser (Picobrite PB-375L) with an excitation wavelength of λ_{exc} = 378 nm and a pulse width <100 ps was used. For absolute measurements of photoluminescence quantum yields at ambient temperature and at 77 K, a Hamamatsu Photonics (C9920-02) system was applied. Doping of polymethylmethacrylate (PMMA) films was performed by dissolving the respective complex (<1 wt%) and the polymer in dichloromethane. After this, the solution was spin-coated onto a quartz-glass plate. All calculations were carried out with Gaussian09.[108] As the functional, B3LYP was used and as the basis set, def2-TZVPP was used. As the starting geometry, the structures obtained from X-ray measurements were used. No symmetry constraints were applied.

The data collection for the single crystal structure determinations was performed on a Stoe IPDS-II or IIT or a Bruker D8 QUEST diffractometer by the X-ray service department of the Fachbereich Chemie, University of Marburg. The Stoe IPDS-II and IIT devices are equipped with a Mo-K_α X-ray source (λ = 0.71073 Å), a graphite mono-chromator and an active imaging plate. Stoe IPDS software (X-AREA) was used for data collection, cell refinement and data reduction, respectively.[109] The D8-QUEST is equipped with a Mo-K_α X-ray micro source (Incotec), a fixed chi goniometer and a PHOTON 100 CMOS detector. Bruker software (Bruker Instrument Service, APEX2, SAINT) was used for data collection, cell refinement and data reduction.[110] The structures were solved with SIR-97[111] or

SHELXS-97,[112] refined with SHELXL-2014[112] and finally validated using PLATON[113] software, all within the WinGX[114] software bundle. Absorption corrections were either applied with WinGX (multi-scan[115] or analytical[116]) or beforehand with the APEX2 software (multi-scan).[117] Compound **C8** was described as a non-merohedral twin. An HKLF5 absorption correction using Stoe X-Red32 (TwinAbs)[109] was applied. Graphic representations were created using Diamond 3.[118] C-bound H-atoms were constrained to the parent site. In all graphics the displacement ellipsoids are shown for the 50% probability level, and hydrogen atoms are shown with arbitrary radius. CCDC 1021437–1021446 contain the supplementary crystallographic data (excluding structure factors) for the structures reported in this paper.

Synthesis of the ligands

Preparation of tris(2-pyridyl)phosphine oxide (tpypo) L1. tpyp (375 mg, 1.4 mmol, 1.0 eq.) was dissolved in toluene (30 mL). After the addition of *t*BuOOH solution (80% in DTBP, 2.0 mL, 16 mmol, 11 eq.), the reaction solution was stirred at room temperature for 5 d and the progress was monitored *via* ^{31}P-NMR spectroscopy. After completion of the reaction, the solvent was removed *in vacuo* and the crude product was triturated with isopropanol (10 mL). After drying *in vacuo*, a colorless powder was obtained. Yield: 372 mg (1.3 mmol, 94%). Anal. Calc. for $C_{15}H_{12}N_3OP$ (281.25 g mol^{-1}) C 64.06, H 4.30, N 14.94%; found C 63.75, H 4.30, N 14.92%. ^{1}H NMR (300.1 MHz, DMSO-d_6): δ (ppm) = 8.74 (dd, $^3J_{65}$ = 4.7 Hz, 3H, H6), 7.90–8.03 (m, 6H, H3/H4), 7.54–7.61 (m, 3H, H5). ^{13}C{^{1}H} (75.5 MHz, DMSO-d_6): δ (ppm) = 154.9 (d, $^1J_{CP}$ = 132.2 Hz, C2), 150.2 (d, $^3J_{CP}$ = 18.9 Hz, C6), 136.4 (d, $^3J_{CP}$ = 9.2 Hz, C4), 128.5 (d, $^2J_{CP}$ = 21.4 Hz, C3), 126.0 (d, $^4J_{CP}$ = 3.1 Hz, C5). ^{31}P{^{1}H} (161.9 MHz, DMSO-d_6): δ (ppm) = 16.43. ^{1}H NMR (300.1 MHz, $CDCl_3$): δ (ppm) = 8.77 (bs, 3H, H6), 8.18 (bs, 3H, H3), 7.79 (bs, 3H, H4), 7.36 (bs, 3H, H5). ^{13}C{^{1}H} (75.5 MHz, $CDCl_3$): δ (ppm) = 154.9 (d, $^1J_{CP}$ = 133.0 Hz, C2), 150.5 (d, $^3J_{CP}$ = 19.3 Hz, C6), 136.0 (d, $^3J_{CP}$ = 9.4 Hz, C4), 128.9 (d, $^2J_{CP}$ = 21.0 Hz, C3), 126.4 (d, $^4J_{CP}$ = 3.3 Hz, C5). ^{31}P{^{1}H} (101.3 MHz, $CDCl_3$): δ (ppm) = 14.65. HRMS (ESI+, MeOH): *m*/*z* (%) = 282.0789 (100, [M + H]$^+$ requires 282.0791), 304.0611 (18, [M + Na]$^+$ requires 304.0610). IR (ATR) ν = 3044 (m), 1573 (m), 1454 (m), 1419 (m), 1281 (m), 1242 (w), 1209 (s), 1145 (m), 1125 (m), 1086 (m), 1043 (m), 989 (s), 788 (m), 780 (m), 769 (m), 749 (s), 737 (s), 619 (w), 542 (vs), 502 (s), 458 (m), 445 (s), 400 (m) cm^{-1}.

Preparation of tris(2-pyridyl)phosphine sulfide (tpyps) L2. tpyps was prepared by a modified literature method.[87,88] Tpyp (1.01 g, 3.80 mmol, 1.0 eq.) was dissolved in degassed toluene (20 mL), and sulfur (134 mg, 4.17 mmol, 1.1 eq.) was added. The suspension was refluxed for 24 h and the completion of the reaction was monitored *via* ^{31}P-NMR spectroscopy. After cooling to room temperature the suspension was filtered *via* a syringe filter and the filtrate was evaporated to dryness *in vacuo*. The crude product was recrystallized from ethanol to give a beige-colored powder. Yield: 517 mg (1.74 mmol, 46%). Anal. Calc. for $C_{15}H_{12}N_3PS$ (297.31 g mol^{-1}) C 60.60, H 4.07, N 14.13, S 10.78%; found C 60.59, H 4.13, N 14.04, S 10.74%. ^{1}H NMR (300.1 MHz, DMSO-d_6): δ (ppm) = 8.69 (d, $^3J_{65}$ = 4.7 Hz, 3H, H6), 8.03–8.11 (m, 3H, H3), 7.98 (dddd, $^3J_{43}$ = 7.7 Hz, $^3J_{45}$ = 7.7 Hz, $^4J_{4P}$ = 4.7 Hz, $^4J_{46}$ = 1.7 Hz, 3H, H4), 7.55 (dddd, $^3J_{54}$ = 7.6 Hz, $^3J_{56}$ = 4.5 Hz, $^5J_{5P}$ = 3.0 Hz, $^4J_{53}$ = 1.3 Hz, 3H, H5). ^{13}C{^{1}H} (75.5 MHz, DMSO-d_6): δ (ppm) = 155.0 (d, $^1J_{CP}$ = 115.2 Hz, C2), 149.8 (d, $^3J_{CP}$ = 19.3 Hz, C6), 136.7 (d, $^3J_{CP}$ = 9.8 Hz, C4), 128.4 (d, $^2J_{CP}$ = 24.7 Hz, C3), 125.5 (d, $^4J_{CP}$ = 3.2 Hz, C5). ^{31}P{^{1}H} (161.9 MHz, DMSO-d_6): δ (ppm) = 35.17. HRMS (ESI+, MeOH): *m*/*z* (%) = 320.0380 (100, [M + Na]$^+$ requires 320.0382), 298.0560 (25, [M + H]$^+$ requires 298.0562). IR (ATR) ν = 3037 (w), 1570 (m), 1448 (m), 1418 (m), 1279 (m), 1235 (w), 1161 (w), 1151 (m), 1131 (m), 1085 (m), 1043 (m), 986 (m), 773 (m), 739 (s), 730 (s), 651 (s), 613 (m), 516 (s), 473 (m), 438 (m), 395 (m) cm^{-1}.

Preparation of tris(2-pyridyl)phosphine selenide (tpypse) L3. tpypse was synthesized using a modified literature method.[88] Tpyp (300 mg, 1.14 mmol, 1.0 eq.) was dissolved in degassed toluene (15 mL) and gray selenium (90 mg, 1.14 mmol, 1.0 eq.) was added. The suspension was refluxed for 4 d and the completion of the reaction was monitored *via* ^{31}P-NMR spectroscopy. After cooling to room temperature the suspension was filtered *via* a syringe filter and the yellow-orange filtrate was evaporated to dryness under vacuum. The crude product was triturated with diethyl ether (15 mL). After drying *in vacuo*, a beige-colored powder was obtained. Yield: 185 mg (0.54 mmol, 47%). Anal. Calc. for $C_{15}H_{12}N_3PSe$ (344.22 g mol^{-1}) C 52.34, H 3.51, N 12.21%; found C 52.55, H 3.67, N 12.01%. ^{1}H NMR (300.1 MHz, DMSO-d_6): δ (ppm) = 8.65–8.72 (m, 3H, H6), 8.11 (ddd, $^3J_{34}$ = 7.6 Hz, $^3J_{3P}$ = 6.4 Hz, 3H, H3), 7.99 (dddd, $^3J_{43}$ = 7.8 Hz, $^3J_{45}$ = 7.8 Hz, $^4J_{4P}$ = 4.8 Hz, $^4J_{46}$ = 1.7 Hz, 3H, H4), 7.54 (dddd, $^3J_{54}$ = 7.8 Hz, $^3J_{56}$ = 4.6 Hz, $^5J_{5P}$ = 3.2 Hz, $^4J_{53}$ = 1.3 Hz, 3H, H5). ^{13}C{^{1}H} (75.5 MHz, DMSO-d_6): δ (ppm) = 154.0 (d, $^1J_{CP}$ = 106.5 Hz, C2), 149.8 (d, $^3J_{CP}$ = 19.1 Hz, C6), 136.8 (d, $^3J_{CP}$ = 10.0 Hz, C4), 128.9 (d, $^2J_{CP}$ = 25.6 Hz, C3), 125.5 (d, $^4J_{CP}$ = 3.2 Hz, C5). ^{31}P{^{1}H} (161.9 MHz, DMSO-d_6): δ (ppm) = 30.58. ^{1}H NMR (300.1 MHz, $CDCl_3$): δ (ppm) = 8.71 (ddd, $^3J_{65}$ = 4.7 Hz, $^4J_{64}$ = 1.7 Hz, 3H, H6), 8.33 (ddd, $^3J_{34}$ = 7.8 Hz, $^3J_{3P}$ = 6.7 Hz, 6H, H3), 7.80 (dddd, $^3J_{43}$ = 7.8 Hz, $^3J_{45}$ = 7.8 Hz, $^4J_{4P}$ = 4.6 Hz, $^4J_{46}$ = 1.8 Hz, 6H, H4), 7.34 (dddd, $^3J_{54}$ = 7.8 Hz, $^3J_{56}$ = 4.6 Hz, $^5J_{5P}$ = 3.1 Hz, $^4J_{53}$ = 1.2 Hz, 3H, H5). ^{13}C{^{1}H} (75.5 MHz, $CDCl_3$): δ (ppm) = 154.5 (d, $^1J_{CP}$ = 106.0 Hz, C2), 150.1 (d, $^3J_{CP}$ = 19.0 Hz, C6), 136.4 (d, $^3J_{CP}$ = 10.4 Hz, C4), 129.5 (d, $^2J_{CP}$ = 26.1 Hz, C3), 125.1 (d, $^4J_{CP}$ = 3.2 Hz, C5). ^{31}P{^{1}H} (101.3 MHz, $CDCl_3$): δ (ppm) = 30.54. HRMS (ESI+, MeOH): *m*/*z* (%) = 367.9826 (100, [M + Na]$^+$ requires 367.9827), 346.0010 (34, [M + H]$^+$ requires 346.0007). IR (ATR) ν = 1570 (m), 1451 (m), 1422 (s), 1287 (m), 1127 (m), 1086 (m), 1052 (m), 988 (s), 906 (m), 770 (a), 738 (a), 730 (m), 715 (m), 619 (w), 560 (vs), 502 (vs), 449 (s), 396 (m) cm^{-1}.

Preparation of tris(2-pyridyl)arsine (tpyas). tpyas was prepared analogously using the following literature procedure.[82] 2-Bromopyridine (10.93 g, 69.2 mmol, 3.9 eq.) was dissolved in diethyl ether (100 mL). After cooling to −78 °C *n*BuLi (2.55 M in *n*-hexane, 28 mL, 71.4 mmol, 4.0 eq.) was added quickly and the solution turned dark red. The solution was first stirred for 1 h at −78 °C followed by stirring for 1 h without cooling bath.

Then the reaction solution was cooled to −100 °C and a solution of arsenic trichloride (1.5 mL, 17.9 mmol, 1.0 eq.) in diethyl ether (50 mL) was added dropwise (5–10 mmol h^{-1}) at a constant temperature before warming slowly to room temperature overnight. The reaction solution turned dark green and a colorless precipitate was formed. After the addition of 2 M HCl (25 mL), the colorless precipitate dissolved. The aqueous phase was isolated and the organic phase was extracted three times with 2 M HCl (25 mL). The aqueous phases were combined and alkalized (pH = 8–10) with a saturated NaOH solution. The formed precipitate was filtered off and washed two times with cold water (10 mL). After drying *in vacuo*, a colorless powder was obtained. Yield: 1.13 g (3.7 mmol, 21%). Anal. Calc. for $C_{15}H_{12}AsN_3$ (309.20 g mol^{-1}) C 58.27, H 3.91, N 13.59%; found C 58.05, H 3.99, N 13.51%. ^{1}H NMR (300.1 MHz, DMSO-d_6): δ (ppm) = 8.66 (ddd, $^3J_{65}$ = 4.8 Hz, $^4J_{64}$ = 1.8 Hz, $^5J_{63}$ = 1.0 Hz, 3H, H6), 7.73 (ddd, $^3J_{43}$ = 7.7 Hz, $^3J_{45}$ = 7.7 Hz, $^4J_{46}$ = 1.9 Hz, 3H, H4), 7.35 (ddd, $^3J_{54}$ = 7.6 Hz, $^3J_{56}$ = 4.8 Hz, $^4J_{53}$ = 1.2 Hz, 3H, H5), 7.29 (ddd, $^3J_{34}$ = 7.7 Hz, $^4J_{35}$ = 1.1 Hz, $^5J_{36}$ = 1.1 Hz, 3H, H3). ^{13}C{^{1}H} (75.5 MHz, DMSO-d_6): δ (ppm) = 165.3 (C2), 150.2 (C6), 136.2 (C4), 128.8 (C3), 123.1 (C5). HRMS (ESI+, MeOH): *m*/*z* (%) = 332.0139 (100, $[M + Na]^+$ requires 332.0139), 310.0317 (36, $[M + H]^+$ requires 310.0320). IR (ATR) ν = 3038 (m), 1568 (s), 1556 (s), 1445 (s), 1418 (s), 1281 (m), 1150 (m), 1112 (m), 1104 (m), 1082 (m), 1043 (m), 988 (s), 755 (vs), 743 (s), 696 (m), 618 (m), 485 (s), 469 (s), 449 (m), 396 (s) cm^{-1}.

Preparation of tris(2-pyridyl)arsine oxide (tpyaso) L4. tpyas (57 mg, 0.18 mmol, 1.0 eq.) was dissolved in toluene (15 mL) and *t*BuOOH solution (80% in DTBP, 0.12 mL, 0.96 mmol, 5.3 eq.) was added. The reaction solution was stirred at room temperature for 5 d. The solvent was removed under vacuum and the crude product was washed with *n*-pentane. After drying *in vacuo*, a colorless powder was obtained. Yield: 51 mg (0.16 mmol, 89%). Anal. Calc. for $C_{15}H_{12}N_3AsO$ (325.20 g mol^{-1}) C 55.40, H 3.72, N 12.92%; found C 55.04, H 3.83, N 12.51%. ^{1}H NMR (300.1 MHz, DMSO-d_6): δ (ppm) = 8.74 (d, $^3J_{65}$ = 4.5 Hz, 3H, H6), 7.92–8.10 (m, 6H, H4/H3), 7.55–7.66 (m, 3H, H5). ^{13}C{^{1}H} (75.5 MHz, DMSO-d_6): δ (ppm) = 157.6 (C2), 150.8 (C6), 137.3 (C4), 128.1 (C3), 126.3 (C5). HRMS (ESI+, MeCN): *m*/*z* (%) = 326.0273 (100, $[M + H]^+$ requires 326.0269). IR (ATR) ν = 3037 (m), 1566 (s), 1449 (s), 1418 (vs), 1282 (m), 1154 (m), 1120 (m), 1083 (m), 1038 (m), 987 (m), 899 (s), 777 (s), 765 (s), 707 (m), 613 (m), 470 (s), 399 (m) cm^{-1}.

General procedure for the copper complexes

The ligand tpypo, tpyps, tpypse, tpyaso or tpym was dissolved in a minimal amount of acetonitrile and CuCl, CuBr or CuI was added. After stirring for 1 d at room temperature the precipitated product was isolated by centrifugation. The supernatant liquid was used for the preparation of single crystals. After a few days of storage at 4 °C, single crystals were obtained.

[CuCltpypo] C1. Prepared from CuCl (35 mg, 0.36 mmol, 1.0 eq.) and tpypo (100 mg, 0.36 mmol, 1.0 eq.) in acetonitrile (5 mL); orange-red powder. Yield: 59 mg (0.16 mmol, 44%). Anal. Calc. for $C_{15}H_{12}N_3POCuCl$ (380.25 g mol^{-1}) C 47.38, H 3.18, N 11.05%; found C 46.75, H 3.16, N 10.81%. ^{1}H NMR (300.1 MHz, $CDCl_3$): δ (ppm) = 9.00–9.06 (m, 3H, H6), 8.39 (ddd, $^3J_{34}$ = 7.7 Hz, $^3J_{3P}$ = 6.6 Hz, 3H, H3), 7.95 (dddd, $^3J_{43}$ = 7.8 Hz, $^3J_{45}$ = 7.8 Hz, $^4J_{4P}$ = 3.9 Hz, $^4J_{46}$ = 1.6 Hz, 3H, H4), 7.52 (dddd, $^3J_{54}$ = 7.8 Hz, $^3J_{56}$ = 5.0 Hz, $^5J_{5P}$ = 1.9 Hz, $^4J_{53}$ = 1.4 Hz, 3H, H5). ^{13}C{^{1}H} (75.5 MHz, $CDCl_3$): δ (ppm) = 151.2 (d, $^3J_{CP}$ = 13.8 Hz, C6), 150.9 (d, $^1J_{CP}$ = 130.1 Hz, C2), 137.0 (d, $^3J_{CP}$ = 9.9 Hz, C4), 129.1 (d, $^2J_{CP}$ = 18.4 Hz, C3), 126.7 (d, $^4J_{CP}$ = 2.9 Hz, C5). ^{31}P{^{1}H} (101.3 MHz, $CDCl_3$): δ (ppm) = −9.79. HRMS (ESI+, MeCN): *m*/*z* (%) = 385.0276 (100, [tpypoCu + MeCN]$^+$ requires 385.0274). IR (ATR) ν = 1578 (w), 1434 (m), 1341 (w), 1275 (w), 1221 (m), 1143 (m), 1079 (w), 1050 (w), 1003 (w), 914 (w), 876 (w), 829 (w), 780 (m), 740 (m), 682 (w), 641 (w), 538 (vs), 455 (m), 410 (m) cm^{-1}.

[CuBrtpypo] C2. Prepared from CuBr (51 mg, 0.36 mmol, 1.0 eq.) and tpypo (100 mg, 0.36 mmol, 1.0 eq.) in acetonitrile (5 mL); orange powder. Yield: 71 mg (0.17 mmol, 47%). Anal. Calc. for $C_{15}H_{12}N_3POCuBr$ (424.70 g mol^{-1}) C 42.42, H 2.85, N 9.89%; found C 42.25, H 2.82, N 9.74%. ^{1}H NMR (300.1 MHz, $CDCl_3$): δ (ppm) = 9.03 (d, $^3J_{65}$ = 4.9 Hz, 3H, H6), 8.39 (dd, $^3J_{34}$ = 7.5 Hz, $^3J_{3P}$ = 6.8 Hz, 3H, H3), 7.96 (dddd, $^3J_{43}$ = 7.8 Hz, $^3J_{45}$ = 7.8 Hz, $^4J_{4P}$ = 3.9 Hz, $^4J_{46}$ = 1.5 Hz 3H, H4), 7.46–7.57 (m, 3H, H5). ^{13}C{^{1}H} (75.5 MHz, $CDCl_3$): δ (ppm) = 151.4 (d, $^3J_{CP}$ = 13.7 Hz, C6), 150.8 (d, $^1J_{CP}$ = 130.0 Hz, C2), 137.1 (d, $^3J_{CP}$ = 9.9 Hz, C4), 129.1 (d, $^2J_{CP}$ = 18.4 Hz, C3), 126.8 (d, $^4J_{CP}$ = 2.9 Hz, C5). ^{31}P{^{1}H} (101.3 MHz, $CDCl_3$): δ (ppm) = −9.29. HRMS (ESI+, MeCN): *m*/*z* (%) = 385.0273 (100, [tpypoCu + MeCN]$^+$ requires 385.0274). IR (ATR) ν = 1579 (w), 1435 (m), 1325 (w), 1275 (w), 1223 (m), 1144 (m), 1080 (w), 1049 (w), 1004 (w), 914 (w), 878 (w), 829 (w), 779 (m), 741 (s), 687 (w), 642 (w), 538 (vs), 454 (m), 411 (m) cm^{-1}.

[CuItpypo] C3. Prepared from CuI (72 mg, 0.38 mmol, 1.0 eq.) and tpypo (106 mg, 0.38 mmol, 1.0 eq.) in acetonitrile (8 mL); orange powder. Yield: 84 mg (0.18 mmol, 47%). Anal. Calc. for $C_{15}H_{12}CuIN_3OP$ (471.71 g mol^{-1}) C 38.19, H 2.56, N 8.91%; found C 38.10, H 2.53, N 8.81%. ^{1}H NMR (300.1 MHz, DMSO-d_6): δ (ppm) = 8.81 (d, $^3J_{65}$ = 4.8 Hz, 3H, H6), 8.36 (dd, 3H, H3), 8.19 (dddd, $^3J_{43}$ = 7.7 Hz, $^3J_{45}$ = 7.7 Hz, $^4J_{4P}$ = 3.8 Hz, $^4J_{46}$ = 1.4 Hz, 3H, H4), 7.72–7.82 (m, 3H, H5). ^{13}C{^{1}H} (75.5 MHz, DMSO-d_6): δ (ppm) = 151.0 (d, $^3J_{CP}$ = 13.1 Hz, C6), 149.9 (d, $^1J_{CP}$ = 127.9 Hz, C2), 138.4 (d, $^3J_{CP}$ = 9.5 Hz, C4), 129.1 (d, $^2J_{CP}$ = 18.2 Hz, C3), 127.5 (d, $^4J_{CP}$ = 2.7 Hz, C5). ^{31}P{^{1}H} (161.9 MHz, DMSO-d_6): δ (ppm) = −7.62. ^{1}H NMR (300.1 MHz, $CDCl_3$): δ (ppm) = 9.05 (ddd, $^3J_{65}$ = 5.0 Hz, $^4J_{64}$ = 1.5 Hz, 3H, H6), 8.40 (dddd, $^3J_{34}$ = 7.7 Hz, $^3J_{3P}$ = 6.6 Hz, 3H, H3), 7.97 (dddd, $^3J_{43}$ = 7.8 Hz, $^3J_{45}$ = 7.8 Hz, $^4J_{4P}$ = 3.8 Hz, $^4J_{46}$ = 1.6 Hz, 3H, H4), 7.54 (dddd, $^3J_{54}$ = 7.9 Hz, $^3J_{56}$ = 5.0 Hz, $^5J_{5P}$ = 2.0 Hz, $^4J_{53}$ = 1.4 Hz, 3H, H5). ^{13}C{^{1}H} (75.5 MHz, $CDCl_3$): δ (ppm) = 152.0 (d, $^3J_{CP}$ = 13.4 Hz, C6), 150.5 (d, $^1J_{CP}$ = 129.8 Hz, C2), 137.3 (d, $^3J_{CP}$ = 9.8 Hz, C4), 129.1 (d, $^2J_{CP}$ = 18.4 Hz, C3), 126.8 (d, $^4J_{CP}$ = 3.0 Hz, C5). ^{31}P{^{1}H} (101.3 MHz, $CDCl_3$): δ (ppm) = −8.08. HRMS (ESI+, MeCN): *m*/*z* (%) = 385.0272 (100, [tpypoCu + MeCN]$^+$ requires 385.0274), 344.0012 (8, [tpypoCu]$^+$ requires 344.0009). IR (ATR) ν = 3046 (m), 1578 (m), 1444 (m), 1430 (m), 1413 (m), 1282 (m), 1250 (m), 1220 (s),

1139 (m), 1125 (m), 1080 (m), 1038 (m), 1005 (m), 777 (m), 748 (s), 732 (s), 638 (w), 540 (vs), 451 (m), 409 (m) cm^{-1}.

[CuCltpyps] C4. Prepared from CuCl (33 mg, 0.34 mmol, 1.0 eq.) and tpyps (100 mg, 0.34 mmol, 1.0 eq.) in acetonitrile (8 mL); red powder. Yield: 89 mg (0.22 mmol, 65%). Anal. Calc. for $C_{15}H_{12}N_3PSCuCl$ (396.31 g mol^{-1}) C 45.46, H 3.05, N 10.60, S 8.09%; found C 44.56, H 3.27, N 10.36, S 7.67%. ^1H NMR (300.1 MHz, DMSO-d_6): δ (ppm) = 8.79 (d, $^3J_{65}$ = 4.7 Hz, 3H, H6), 8.55 (dd, 3H, H3), 8.19 (dddd, $^3J_{43}$ = 7.8 Hz, $^3J_{45}$ = 7.8 Hz, $^4J_{4P}$ = 4.4 Hz, $^4J_{46}$ = 1.7 Hz, 3H, H4), 7.75 (dddd, $^3J_{54}$ = 7.7 Hz, $^3J_{56}$ = 4.9 Hz, $^4J_{5P}$ = 2.6 Hz, $^4J_{53}$ = 1.2 Hz, 3H, H5). $^{13}C\{^1H\}$ (75.5 MHz, DMSO-d_6): δ (ppm) = 150.4 (d, $^3J_{CP}$ = 13.7 Hz, C6), 150.1 (d, $^1J_{CP}$ = 108.0 Hz, C2), 138.3 (d, $^3J_{CP}$ = 10.8 Hz, C4), 129.2 (d, $^2J_{CP}$ = 24.3 Hz, C3), 127.2 (d, $^4J_{CP}$ = 2.8 Hz, C5). $^{31}P\{^1H\}$ (161.9 MHz, DMSO-d_6): δ (ppm) = 14.71. ^1H NMR (300.1 MHz, $CDCl_3$): δ (ppm) = 9.00–9.06 (m, 3H, H6), 8.73 (ddd, $^3J_{3P}$ = 8.8 Hz, $^3J_{34}$ = 7.9 Hz, 3H, H3), 7.95 (dddd, $^3J_{43}$ = 7.8 Hz, $^3J_{45}$ = 7.8 Hz, $^4J_{4P}$ = 4.2 Hz, $^4J_{46}$ = 1.7 Hz, 3H, H4), 7.50 (dddd, $^3J_{54}$ = 7.6 Hz, $^3J_{56}$ = 4.9 Hz, $^5J_{5P}$ = 2.4 Hz, $^4J_{53}$ = 1.3 Hz, 3H, H5). $^{13}C\{^1H\}$ (75.5 MHz, $CDCl_3$): δ (ppm) = 150.7 (d, $^3J_{CP}$ = 12.5 Hz, C6), 150.6 (d, $^1J_{CP}$ = 108.3 Hz, C2), 137.1 (d, $^3J_{CP}$ = 11.6 Hz, C4), 129.5 (d, $^2J_{CP}$ = 24.6 Hz, C3), 126.3 (d, $^4J_{CP}$ = 3.0 Hz, C5). $^{31}P\{^1H\}$ (121.5 MHz, $CDCl_3$): δ (ppm) = 9.10. HRMS (ESI+, MeCN): *m*/*z* (%) = 401.0049 (100, $[tpypsCu + MeCN]^+$ requires 401.0046), 359.9784 (2, $[tpypsCu]^+$ requires 359.9780). IR (ATR) ν = 1574 (m), 1439 (m), 1426 (m), 1279 (m), 1245 (w), 1152 (w), 1127 (m), 1080 (m), 1045 (m), 1002 (m), 771 (m), 739 (s), 727 (m), 661 (s), 634 (m), 518 (vs), 435 (m), 408 (m), 382 (w) cm^{-1}.

[CuBrtpyps] C5. Prepared from CuBr (49 mg, 0.34 mmol, 1.0 eq.) and tpyps (100 mg, 0.34 mmol, 1.0 eq.) in acetonitrile (8 mL); bright red powder. Yield: 99 mg (0.22 mmol, 65%). Anal. Calc. for $C_{15}H_{12}N_3PSCuBr$ (440.77 g mol^{-1}) C 40.88, H 2.74, N 9.53, S 7.27%; found C 40.52, H 2.87, N 9.50, S 6.89%. ^1H NMR (300.1 MHz, DMSO-d_6): δ (ppm) = 8.78–8.85 (m, 3H, H6), 8.65 (dd, 3H, H3), 8.21 (dddd, $^3J_{43}$ = 7.9 Hz, $^3J_{45}$ = 7.9 Hz, $^4J_{4P}$ = 4.3 Hz, $^4J_{46}$ = 1.7 Hz, 3H, H4), 7.77 (dddd, $^3J_{54}$ = 7.6 Hz, $^3J_{56}$ = 4.9 Hz, $^5J_{5P}$ = 2.5 Hz, $^4J_{53}$ = 1.3 Hz, 3H, H5). $^{13}C\{^1H\}$ (100.6 MHz, DMSO-d_6): δ (ppm) = 150.4 (d, $^3J_{CP}$ = 12.4 Hz, C6), 149.6 (d, $^1J_{CP}$ = 107.4 Hz, C2), 138.4 (d, $^3J_{CP}$ = 11.0 Hz, C4), 129.2 (d, $^2J_{CP}$ = 24.5 Hz, C3), 127.2 (d, $^4J_{CP}$ = 1.3 Hz, C5). $^{31}P\{^1H\}$ (161.9 MHz, DMSO-d_6): δ (ppm) = 11.96. ^1H NMR (300.1 MHz, $CDCl_3$): δ (ppm) = 9.00–9.06 (m, 3H, H6), 8.74 (ddd, $^3J_{3P}$ = 8.8 Hz, $^3J_{34}$ = 7.8 Hz, 3H, H3), 7.95 (dddd, $^3J_{43}$ = 7.8 Hz, $^3J_{45}$ = 7.8 Hz, $^4J_{4P}$ = 4.2 Hz, $^4J_{46}$ = 1.7 Hz, 3H, H4), 7.51 (dddd, $^3J_{54}$ = 7.6 Hz, $^3J_{56}$ = 4.9 Hz, $^5J_{5P}$ = 2.5 Hz, $^4J_{53}$ = 1.3 Hz, 3H, H5). $^{13}C\{^1H\}$ (75.5 MHz, $CDCl_3$): δ (ppm) = 151.0 (d, $^3J_{CP}$ = 12.2 Hz, C6), 150.5 (d, $^1J_{CP}$ = 108.2 Hz, C2), 137.2 (d, $^3J_{CP}$ = 11.5 Hz, C4), 129.5 (d, $^2J_{CP}$ = 24.6 Hz, C3), 126.4 (d, $^4J_{CP}$ = 3.0 Hz, C5). $^{31}P\{^1H\}$ (121.5 MHz, $CDCl_3$): δ (ppm) = 9.67. HRMS (ESI+, MeCN): *m*/*z* (%) = 401.0042 (100, $[tpypsCu + MeCN]^+$ requires 401.0046). IR (ATR) ν = 1574 (m), 1440 (m), 1426 (m), 1279 (m), 1153 (w), 1126 (m), 1081 (m), 1044 (m), 1003 (m), 771 (m), 739 (s), 726 (m), 661 (s), 634 (m), 518 (vs), 436 (m), 408 (m), 382 (m) cm^{-1}.

[CuItpyps] C6. Prepared from CuI (66 mg, 0.35 mmol, 1.0 eq.) and tpyps (104 mg, 0.35 mmol, 1.0 eq.) in acetonitrile (8 mL); orange-red powder. Yield: 97 mg (0.20 mmol, 57%). Anal. Calc. for $C_{15}H_{12}N_3PSCuI$ (487.77 g mol^{-1}) C 36.94, H 2.48, N 8.61, S 6.57%; found C 36.77, H 2.47, N 8.60, S 6.62%. ^1H NMR (300.1 MHz, DMSO-d_6): δ (ppm) = 8.84 (d, $^3J_{65}$ = 4.9 Hz, 3H, H6), 8.68 (dd, 3H, H3), 8.23 (tdd, $^3J_{43}$ = 7.8 Hz, $^3J_{45}$ = 7.8 Hz, $^4J_{4P}$ = 4.2 Hz, $^3J_{46}$ = 1.6 Hz, 3H, H4), 7.79 (dddd, $^3J_{54}$ = 7.6 Hz, $^3J_{56}$ = 4.8 Hz, $^5J_{5P}$ = 2.4 Hz, $^4J_{53}$ = 1.2 Hz, 3H, H5). $^{13}C\{^1H\}$ (75.5 MHz, DMSO-d_6): δ (ppm) = 150.8 (d, $^3J_{CP}$ = 12.1 Hz, C6), 149.2 (d, $^1J_{CP}$ = 107.5 Hz, C2), 138.6 (d, $^3J_{CP}$ = 11.0 Hz, C4), 129.3 (d, $^2J_{CP}$ = 24.3 Hz, C3), 127.3 (d, $^4J_{CP}$ = 2.8 Hz, C5). $^{31}P\{^1H\}$ (161.9 MHz, DMSO-d_6): δ (ppm) = 12.36. ^1H NMR (300.1 MHz, $CDCl_3$): δ (ppm) = 9.06 (ddd, $^3J_{65}$ = 5.0 Hz, $^4J_{64}$ = 1.7 Hz, 3H, H6), 8.71–8.79 (ddd, $^3J_{3P}$ = 8.9 Hz, $^3J_{34}$ = 7.7 Hz, 3H, H3), 7.96 (dddd, $^3J_{43}$ = 7.8 Hz, $^3J_{45}$ = 7.8 Hz, $^4J_{4P}$ = 4.1 Hz, $^4J_{46}$ = 1.7 Hz, 3H, H4), 7.52 (dddd, $^3J_{54}$ = 7.6 Hz, $^3J_{56}$ = 5.0 Hz, $^5J_{5P}$ = 2.5 Hz, $^4J_{53}$ = 1.3 Hz, 3H, H5). $^{13}C\{^1H\}$ (75.5 MHz, $CDCl_3$): δ (ppm) = 151.5 (d, $^3J_{CP}$ = 12.0 Hz, C6), 150.3 (d, $^1J_{CP}$ = 107.9 Hz, C2), 137.4 (d, $^3J_{CP}$ = 11.5 Hz, C4), 129.5 (d, $^2J_{CP}$ = 24.6 Hz, C3), 126.4 (d, $^4J_{CP}$ = 3.0 Hz, C5). $^{31}P\{^1H\}$ (101.3 MHz, $CDCl_3$): δ (ppm) = 11.47. HRMS (ESI+, MeCN): *m*/*z* (%) = 401.0048 (100, $[tpypsCu + MeCN]^+$ requires 401.0046), 359.9786 (2, $[tpypsCu]^+$ requires 359.9780). IR (ATR) ν = 1574 (m), 1442 (m), 1425 (m), 1364 (w), 1277 (w), 1245 (w), 1150 (w), 1126 (w), 1080 (w), 1045 (w), 1004 (m), 906 (w), 786 (m), 771 (m), 740 (s), 725 (m), 664 (s), 635 (m), 518 (vs), 445 (w), 434 (w), 413 (m), 384 (m) cm^{-1}.

[CuItpypse] C7. Prepared from CuI (56 mg, 0.29 mmol, 1.0 eq.) and tpypse (101 mg, 0.29 mmol, 1.0 eq.) in acetonitrile (8 mL); orange-red powder. Yield: 25 mg (0.05 mmol, 17%). Anal. Calc. for $C_{15}H_{12}CuIN_3PSe$ (534.67 g mol^{-1}) C 33.70, H 2.26, N 7.86%; found C 33.52, H 2.35, N 7.69%. ^1H NMR (500.2 MHz, DMSO-d_6): δ (ppm) = 8.84 (d, $^3J_{65}$ = 4.8 Hz, 3H, H6), 8.79 (dd, 3H, H3), 8.23 (dddd, $^3J_{43}$ = 7.8 Hz, $^3J_{45}$ = 7.8 Hz, $^4J_{4P}$ = 4.3 Hz, $^4J_{46}$ = 1.6 Hz, 3H, H4), 7.78 (dddd, 3H, H5). $^{13}C\{^1H\}$ (75.5 MHz, DMSO-d_6): δ (ppm) = 150.7 (d, $^3J_{CP}$ = 11.3 Hz, C6), 147.9 (d, $^1J_{CP}$ = 97.2 Hz, C2), 138.7 (d, $^3J_{CP}$ = 11.6 Hz, C4), 130.3 (d, $^2J_{CP}$ = 26.5 Hz, C3), 127.3 (d, $^4J_{CP}$ = 2.8 Hz, C5). $^{31}P\{^1H\}$ (202.5 MHz, DMSO-d_6): δ (ppm) = 10.71. ^1H NMR (300.1 MHz, $CDCl_3$): δ (ppm) = 9.03–9.09 (m, 3H, H6), 8.89 (ddd, 3H, H3), 7.96 (dddd, $^3J_{43}$ = 7.8 Hz, $^3J_{45}$ = 7.8 Hz, $^4J_{4P}$ = 4.2 Hz, $^4J_{46}$ = 1.7 Hz, 3H, H4), 7.51 (dddd, $^3J_{54}$ = 7.7 Hz, $^3J_{56}$ = 4.9 Hz, $^5J_{5P}$ = 2.6 Hz, $^4J_{53}$ = 1.3 Hz, 3H, H5). $^{13}C\{^1H\}$ (75.5 MHz, $CDCl_3$): δ (ppm) = 151.4 (d, $^3J_{CP}$ = 11.3 Hz, C6), 148.9 (d, $^1J_{CP}$ = 97.4 Hz, C2), 137.5 (d, $^3J_{CP}$ = 12.1 Hz, C4), 130.7 (d, $^2J_{CP}$ = 27.0 Hz, C3), 126.4 (d, $^4J_{CP}$ = 3.0 Hz, C5). $^{31}P\{^1H\}$ (101.3 MHz, $CDCl_3$): δ (ppm) = 12.07. HRMS (ESI+, CH_2Cl_2): *m*/*z* (%) = 407.9227 (18, $[tpypseCu]^+$ requires 407.9224). IR (ATR) ν = 1573 (m), 1441 (m), 1423 (m), 1363 (w), 1277 (m), 1244 (w), 1150 (w), 1121 (w), 1079 (m), 1046 (m), 1003 (m), 905 (w), 784 (m), 770 (m), 739 (m), 719 (m), 665 (w), 635 (w), 576 (vs), 513 (vs), 441 (w), 427 (m), 411 (m) cm^{-1}.

[CuItpyaso] C8. Prepared from CuI (30 mg, 0.16 mmol, 1.0 eq.) and tpyaso (51 mg, 0.16 mmol, 1.0 eq.) in acetonitrile (8 mL); yellow powder. Yield: 49 mg (0.10 mmol, 62%). Anal. Calc. for $C_{15}H_{12}N_3AsOCuI$ (515.65 g mol^{-1}) C 34.94, H 2.35, N 8.15%; found C 34.79, H 2.35, N 8.09%. ^1H NMR

(300.1 MHz, DMSO-d_6): δ (ppm) = 8.79 (d, $^3J_{65}$ = 4.9 Hz, 3H, H6), 8.15–8.24 (m, 3H, H3/H4), 7.71–7.82 (m, 3H, H5). $^{13}C\{^1H\}$ (75.5 MHz, DMSO-d_6): δ (ppm) = 154.7 (C2), 151.2 (C6), 139.0 (C4), 128.0 (C3), 127.5 (C5). ^1H NMR (300.1 MHz, $CDCl_3$): δ (ppm) = 9.06 (ddd, $^3J_{65}$ = 5.0 Hz, $^5J_{63}$ = 0.9 Hz, 3H, H6), 8.28 (dd, $^3J_{34}$ = 7.7 Hz, 3H, H3), 7.99 (ddd, $^3J_{43}$ = 7.7 Hz, $^3J_{45}$ = 7.7 Hz, $^4J_{46}$ = 1.7 Hz, 3H, H4), 7.56 (ddd, $^3J_{54}$ = 7.8 Hz, $^3J_{56}$ = 5.1 Hz, $^4J_{53}$ = 1.3 Hz, 3H, H5). $^{13}C\{^1H\}$ (75.5 MHz, $CDCl_3$): δ (ppm) = 154.6 (C2), 152.5 (C6), 138.1 (C4), 128.0 (C3), 127.2 (C5). HRMS (ESI+, MeCN): *m*/*z* (%) = 428.9750 (93, $[tpyasoCu + MeCN]^+$ requires 428.9752), 387.9489 (9, $[tpyasoCu]^+$ requires 304.0610). IR (ATR) ν = 3046 (w), 1577 (m), 1556 (w), 1444 (m), 1429 (m), 1414 (m), 1371 (w), 1270 (w), 1242 (w), 1154 (w), 1140 (w), 1117 (w), 1043 (m), 1004 (m), 914 (s), 796 (m), 770 (s), 761 (s), 706 (w), 634 (w), 479 (vs), 410 (s) cm^{-1}.

[CuItpym] C9. Prepared from CuI (39 mg, 0.20 mmol, 1.0 eq.) and tpym (50 mg, 0.20 mmol, 1.0 eq.) in acetonitrile (15 mL); bright yellow powder. Yield: 64 mg (0.15 mmol, 75%). Anal. Calc. for $C_{16}H_{13}CuIN_3$ (437.75 g mol^{-1}) C 43.90, H 2.99, N 9.60%; found C 43.81, H 2.96, N 9.68%. ^1H NMR (300.1 MHz, $CDCl_3$): δ (ppm) = 8.83 (d, 3H, H6), 7.64–7.74 (m, 3H, H4), 7.55 (d, 3H, H3), 7.20–7.25 (m, 3H, H5), 5.57 (s, 1H, H7). $^{13}C\{^1H\}$ (75.5 MHz, $CDCl_3$): δ (ppm) = 154.1 (C2), 150.8 (C6), 137.7 (C4), 124.6 (C3), 123.4 (C5), 60.0 (C7). HRMS (ESI+, MeCN): *m*/*z* (%) = 351.0664 (100, $[tpymCu + MeCN]^+$ requires 351.0665), 436.9448 (2, $[M]^+$ requires 436.9445). IR (ATR) ν = 1592 (w), 1466 (w), 1434 (m), 1347 (w), 1187 (w), 1155 (w), 1083 (w), 1054 (w), 1013 (w), 960 (w), 914 (w), 878 (w), 832 (m), 782 (m), 751 (m), 692 (w), 645 (w), 616 (m), 553 (m), 500 (w), 464 (w), 418 (m) cm^{-1}.

Acknowledgements

The authors thank the German Ministry of Education and Research (BMBF) and the German Association of Chemical Industry (Verband der chemischen Industrie, VCI) for financial support.

Notes and references

1 C. Kutal, *Coord. Chem. Rev.*, 1990, **99**, 213–252.
2 O. Horváth, *Coord. Chem. Rev.*, 1994, **135–136**, 303–324.
3 V. W.-W. Yam, K. K.-W. Lo, W. K.-M. Fung and C.-R. Wang, *Coord. Chem. Rev.*, 1998, **171**, 17–41.
4 P. C. Ford, E. Cariati and J. Bourassa, *Chem. Rev.*, 1999, **99**, 3625–3647.
5 V. W.-W. Yam and K. K.-W. Lo, *Chem. Soc. Rev.*, 1999, **28**, 323–334.
6 D. V. Scaltrito, D. W. Thompson, J. A. O'Callaghan and G. J. Meyer, *Coord. Chem. Rev.*, 2000, **208**, 243–266.
7 P. G. Graham, R. D. Pike, M. Sabat, R. D. Bailey and W. T. Pennington, *Inorg. Chem.*, 2000, **39**, 5121–5132.
8 A. Vogler and H. Kunkely, *Top. Curr. Chem.*, 2001, **213**, 143–182.
9 N. Armaroli, *Chem. Soc. Rev.*, 2001, **30**, 113–124.
10 N. Armaroli, G. Accorsi, F. Cardinali and A. Listorti, *Top. Curr. Chem.*, 2007, **280**, 69–115.
11 K. Tsuge, *Chem. Lett.*, 2013, **42**, 204–208.
12 G. Blasse and D. R. McMillin, *Chem. Phys. Lett.*, 1980, **70**, 1–3.
13 Q. Zhang, Q. Zhou, Y. Cheng, L. Wang, D. Ma, X. Jing and F. Wang, *Adv. Mater.*, 2004, **16**, 432–436.
14 N. Armaroli, G. Accorsi, M. Holler, O. Moudam, J.-F. Nierengarten, Z. Zhou, R. T. Wegh and R. Welter, *Adv. Mater.*, 2006, **18**, 1313–1316.
15 G. Che, Z. Su, W. Li, B. Chu, M. Li, Z. Hu and Z. Zhang, *Appl. Phys. Lett.*, 2006, **89**, 103511.
16 Q. Zhang, Q. Zhou, Y. Cheng, L. Wang, D. Ma, X. Jing and F. Wang, *Adv. Funct. Mater.*, 2006, **16**, 1203–1208.
17 A. Tsuboyama, K. Kuge, M. Furugori, S. Okada, M. Hoshino and K. Ueno, *Inorg. Chem.*, 2007, **46**, 1992–2001.
18 Q. Zhang, J. Ding, Y. Cheng, L. Wang, Z. Xie, X. Jing and F. Wang, *Adv. Funct. Mater.*, 2007, **17**, 2983–2990.
19 J. C. Deaton, S. C. Switalski, D. Y. Kondakov, R. H. Young, T. D. Pawlik, D. J. Giesen, S. B. Harkins, A. J. M. Miller, S. F. Mickenberg and J. C. Peters, *J. Am. Chem. Soc.*, 2010, **132**, 9499–9508.
20 M. Hashimoto, S. Igawa, M. Yashima, I. Kawata, M. Hoshino and M. Osawa, *J. Am. Chem. Soc.*, 2011, **133**, 10348–10351.
21 Z. Liu, M. F. Qayyum, C. Wu, M. T. Whited, P. I. Djurovich, K. O. Hodgson, B. Hedman, E. I. Solomon and M. E. Thompson, *J. Am. Chem. Soc.*, 2011, **133**, 3700–3703.
22 A. Wada, Q. Zhang, T. Yasuda, I. Takasu, S. Enomoto and C. Adachi, *Chem. Commun.*, 2012, **48**, 5340–5342.
23 Q. Zhang, T. Komino, S. Huang, S. Matsunami, K. Goushi and C. Adachi, *Adv. Funct. Mater.*, 2012, **22**, 2327–2336.
24 S. Igawa, M. Hashimoto, I. Kawata, M. Yashima, M. Hoshino and M. Osawa, *J. Mater. Chem. C*, 2013, **1**, 542–551.
25 X.-L. Chen, R. Yu, Q.-K. Zhang, L.-J. Zhou, X.-Y. Wu, Q. Zhang and C.-Z. Lu, *Chem. Mater.*, 2013, **25**, 3910–3920.
26 Z. Liu, J. Qiu, F. Wei, J. Wang, X. Liu, M. G. Helander, S. Rodney, Z. Wang, Z. Bian, Z. Lu, M. E. Thompson and C. Huang, *Chem. Mater.*, 2014, **26**, 2368–2373.
27 D. M. Zink, D. Volz, T. Baumann, M. Mydlak, H. Flügge, J. Friedrichs, M. Nieger and S. Bräse, *Chem. Mater.*, 2013, **25**, 4471–4486.
28 R. Czerwieniec, K. Kowalski and H. Yersin, *Dalton Trans.*, 2013, **42**, 9826–9830.
29 M. J. Leitl, F.-R. Küchle, H. A. Mayer, L. Wesemann and H. Yersin, *J. Phys. Chem. A*, 2013, **117**, 11823–11836.
30 D. M. Zink, M. Bächle, T. Baumann, M. Nieger, M. Kühn, C. Wang, W. Klopper, U. Monkowius, T. Hofbeck, H. Yersin and S. Bräse, *Inorg. Chem.*, 2013, **52**, 2292–2305.
31 C. L. Linfoot, M. J. Leitl, P. Richardson, A. F. Rausch, O. Chepelin, F. J. White, H. Yersin and N. Robertson, *Inorg. Chem.*, 2014, **53**, 10854–10861.

32 R. Czerwieniec, J. Yu and H. Yersin, *Inorg. Chem.*, 2011, **50**, 8293–8301.
33 C. A. Parker and C. G. Hatchard, *Trans. Faraday Soc.*, 1961, **57**, 1894–1904.
34 H. Yersin, A. F. Rausch, R. Czerwieniec, T. Hofbeck and T. Fischer, *Coord. Chem. Rev.*, 2011, **255**, 2622–2652.
35 H. Yersin, A. F. Rausch and R. Czerwieniec, Organometallic Emitters for OLEDs: Triplet Harvesting, Singlet Harvesting, Case Structures, and Trends, in *Physics of Organic Semiconductors*, ed. W. Brütting and C. Adachi, Wiley-VCH Verlag, 2012, pp. 371–424.
36 H. Yersin, M. J. Leitl and R. Czerwieniec, *Proc. SPIE*, 2014, **9183**, 22–21.
37 M. J. Leitl, V. A. Krylova, P. I. Djurovich, M. E. Thompson and H. Yersin, *J. Am. Chem. Soc.*, 2014, **136**, 16032–16038.
38 P.-T. Chou and Y. Chi, *Chem. – Eur. J.*, 2007, **13**, 380–395.
39 S. Kappaun, C. Slugovc and E. J. W. List, *Int. J. Mol. Sci.*, 2008, **9**, 1527–1547.
40 J. A. G. Williams, S. Develay, D. L. Rochester and L. Murphy, *Coord. Chem. Rev.*, 2008, **252**, 2596–2611.
41 C. Ulbricht, B. Beyer, C. Friebe, A. Winter and U. S. Schubert, *Adv. Mater.*, 2009, **21**, 4418–4441.
42 Y. You and S. Y. Park, *Dalton Trans.*, 2009, 1267–1282.
43 Y. Chi and P.-T. Chou, *Chem. Soc. Rev.*, 2010, **39**, 638–655.
44 G. M. Farinola and R. Ragni, *Chem. Soc. Rev.*, 2011, **40**, 3467–3482.
45 J. Kalinowski, V. Fattori, M. Cocchi and J. A. G. Williams, *Coord. Chem. Rev.*, 2011, **255**, 2401–2425.
46 T. Hu, L. He, L. Duan and Y. Qiu, *J. Mater. Chem.*, 2012, **22**, 4206–4215.
47 R. D. Costa, E. Ortí, H. J. Bolink, F. Monti, G. Accorsi and N. Armaroli, *Angew. Chem., Int. Ed.*, 2012, **124**, 8300–8334.
48 C.-L. Ho and W.-Y. Wong, *New J. Chem.*, 2013, **37**, 1665–1683.
49 C.-L. Ho, H. Li and W.-Y. Wong, *J. Organomet. Chem.*, 2014, **751**, 261–285.
50 *Highly Efficient OLEDs with Phosphorescent Materials*, ed. H. Yersin, Wiley-VCH, Weinheim, Germany, 2008.
51 A. Bossi, A. F. Rausch, M. J. Leitl, R. Czerwieniec, M. T. Whited, P. I. Djurovich, H. Yersin and M. E. Thompson, *Inorg. Chem.*, 2013, **52**, 12403–12415.
52 J. Brooks, Y. Babayan, S. Lamansky, P. I. Djurovich, I. Tsyba, R. Bau and M. E. Thompson, *Inorg. Chem.*, 2002, **41**, 3055–3066.
53 S. Lamansky, P. Djurovich, D. Murphy, F. Abdel-Razzaq, H.-E. Lee, C. Adachi, P. E. Burrows, S. R. Forrest and M. E. Thompson, *J. Am. Chem. Soc.*, 2001, **123**, 4304–4312.
54 A. Barbieri, G. Accorsi and N. Armaroli, *Chem. Commun.*, 2008, 2185–2193.
55 D. Felder, J.-F. Nierengarten, F. Barigelletti, B. Ventura and N. Armaroli, *J. Am. Chem. Soc.*, 2001, **123**, 6291–6299.
56 Z. A. Siddique, Y. Yamamoto, T. Ohno and K. Nozaki, *Inorg. Chem.*, 2003, **42**, 6366–6378.
57 V. Kalsani, M. Schmittel, A. Listorti, G. Accorsi and N. Armaroli, *Inorg. Chem.*, 2006, **45**, 2061–2067.
58 A. Robertazzi, A. Magistrato, P. de Hoog, P. Carloni and J. Reedijk, *Inorg. Chem.*, 2007, **46**, 5873–5881.
59 A. Lavie-Cambot, M. Cantuel, Y. Leydet, G. Jonusauskas, D. M. Bassani and N. D. McClenaghan, *Coord. Chem. Rev.*, 2008, **252**, 2572–2584.
60 L.-Y. Zhou, M.-S. Ma, Z.-L. Zhang, H. Li, Y.-X. Cheng and A.-M. Ren, *Org. Electron.*, 2012, **13**, 2627–2638.
61 O. Moudam, A. Kaeser, B. Delavaux-Nicot, C. Duhayon, M. Holler, G. Accorsi, N. Armaroli, I. Séguy, J. Navarro, P. Destruel and J.-F. Nierengarten, *Chem. Commun.*, 2007, 3077–3079.
62 R. Venkateswaran, M. S. Balakrishna, S. M. Mobin and H. M. Tuononen, *Inorg. Chem.*, 2007, **46**, 6535–6541.
63 G. Accorsi, N. Armaroli, B. Delavaux-Nicot, A. Kaeser, M. Holler, J.-F. Nierengarten and A. D. Esposti, *J. Mol. Struct. (THEOCHEM)*, 2010, **962**, 7–14.
64 S.-M. Kuang, D. G. Cuttell, D. R. McMillin, P. E. Fanwick and R. A. Walton, *Inorg. Chem.*, 2002, **41**, 3313–3322.
65 K. Saito, T. Arai, N. Takahashi, T. Tsukuda and T. Tsubomura, *Dalton Trans.*, 2006, 4444–4448.
66 I. Andrés-Tomé, J. Fyson, F. B. Dias, A. P. Monkman, G. Iacobellis and P. Coppo, *Dalton Trans.*, 2012, **41**, 8669–8674.
67 D. R. McMillin, J. R. Kirchhoff and K. V. Goodwin, *Coord. Chem. Rev.*, 1985, **64**, 83–92.
68 T. S. Teets, D. V. Partyka, A. J. Esswein, J. B. Updegraff III, M. Zeller, A. D. Hunter and T. G. Gray, *Inorg. Chem.*, 2007, **46**, 6218–6220.
69 K. J. Lotito and J. C. Peters, *Chem. Commun.*, 2010, **46**, 3690–3692.
70 V. A. Krylova, P. I. Djurovich, M. T. Whited and M. E. Thompson, *Chem. Commun.*, 2010, **46**, 6696–6698.
71 V. A. Krylova, P. I. Djurovich, J. W. Aronson, R. Haiges, M. T. Whited and M. E. Thompson, *Organometallics*, 2012, **31**, 7983–7993.
72 M. Osawa, *Chem. Commun.*, 2014, **50**, 1801–1803.
73 V. A. Krylova, P. I. Djurovich, B. L. Conley, R. Haiges, M. T. Whited, T. J. Williams and M. E. Thompson, *Chem. Commun.*, 2014, **50**, 7176–7179.
74 P. Aslanidis, P. J. Cox, S. Divanidis and A. C. Tsipis, *Inorg. Chem.*, 2002, **41**, 6875–6886.
75 H. Araki, K. Tsuge, Y. Sasaki, S. Ishizaka and N. Kitamura, *Inorg. Chem.*, 2005, **44**, 9667–9675.
76 T. Tsukuda, A. Nakamura, T. Arai and T. Tsubomura, *Bull. Chem. Soc. Jpn.*, 2006, **79**, 288–290.
77 A. Tsuboyama, K. Kuge, M. Furugori, S. Okada, M. Hoshino and K. Ueno, *Inorg. Chem.*, 2007, **46**, 1992–2001.
78 H. Araki, K. Tsuge, Y. Sasaki, S. Ishizaka and N. Kitamura, *Inorg. Chem.*, 2007, **46**, 10032–10034.
79 S. B. Harkins, N. P. Mankad, A. J. M. Miller, R. K. Szilagyi and J. C. Peters, *J. Am. Chem. Soc.*, 2008, **130**, 3478–3485.
80 A. Acosta, J. I. Zink and J. Cheon, *Inorg. Chem.*, 2000, **39**, 427–432.
81 V. Pawlowski, G. Knör, C. Lennartz and A. Vogler, *Eur. J. Inorg. Chem.*, 2005, 3167–3171.

82 F. R. Keene, M. R. Snow, P. J. Stephenson and E. R. T. Tiekink, *Inorg. Chem.*, 1988, **27**, 2040–2045.
83 K. Kurtev, D. Ribola, R. A. Jones, D. J. Cole-Hamilton and G. Wilkinson, *J. Chem. Soc., Dalton Trans.*, 1980, 55–58.
84 S. F. Malysheva, A. O. Korocheva, N. A. Belogorlova, A. V. Artemév, N. K. Gusarova and B. A. Trofimov, *Dokl. Chem.*, 2012, **445**, 164–165.
85 S. F. Malysheva, A. V. Artemév, N. A. Belogorlova, A. O. Korocheva, N. K. Gusarova and B. A. Trofimov, *Russ. J. Gen. Chem.*, 2012, **82**, 1307–1308.
86 B. A. Trofimov, N. K. Gusarova, A. V. Artemév, S. F. Malysheva, N. A. Belogorlova, A. O. Korocheva, O. N. Kazheva, G. G. Alexandrov and O. A. Dyachenko, *Mendeleev Commun.*, 2012, **22**, 187–188.
87 F. G. Mann and J. Watson, *J. Org. Chem.*, 1948, **13**, 502–531.
88 A. N. Kharat, A. Bakhoda, T. Hajiashrafi and A. Abbasi, *Phosphorus, Sulfur Silicon Relat. Elem.*, 2010, **185**, 2341–2347.
89 Y. Uchida, K. Matsuoka, R. Kajita, Y. Kawasaki and S. Oae, *Heteroat. Chem.*, 1997, **8**, 439–449.
90 F. R. Keene, P. J. Stephenson and E. R. T. Tiekink, *Inorg. Chim. Acta*, 1991, **187**, 217–220.
91 A. Maleckis, J. W. Kampf and M. S. Sanford, *J. Am. Chem. Soc.*, 2013, **135**, 6618–6625.
92 K. A. Al-Farhan, *J. Crystallogr. Spectrosc.*, 1992, **22**, 687–689.
93 P. W. Codding and K. A. Kerr, *Acta Crystallogr., Sect. B: Struct. Crystallogr. Cryst. Chem.*, 1978, **34**, 3785–3787.
94 A. Jesser, M. Rohrmüller, W. G. Schmidt and S. Herres-Pawlis, *J. Comput. Chem.*, 2014, **35**, 1–17.
95 N. Kitajima, K. Fujisawa, M. Tanaka and Y. Moro-oka, *J. Am. Chem. Soc.*, 1992, **114**, 9232–9233.
96 K. Fujisawa, K. Fujita, T. Takahashi, N. Kitajima, Y. Moro-oka, Y. Mastunaga, Y. Miyashita and K. Okamoto, *Inorg. Chem. Commun.*, 2004, **7**, 1188–1190.
97 K. L. McCall, J. R. Jennings, H. Wang, A. Morandeira, L. M. Peter, J. R. Durrant, L. J. Yellowlees, J. D. Woollins and N. Robertson, *J. Photochem. Photobiol., A*, 2009, **202**, 196–204.
98 A. Vlček Jr. and S. Záliš, *Coord. Chem. Rev.*, 2007, **251**, 258–287.
99 W. Siebrand, *J. Chem. Phys.*, 1967, **46**, 440–447.
100 G. W. Robinson and R. P. Frosch, *J. Chem. Phys.*, 1963, **38**, 1187–1203.
101 A. F. Rausch, M. E. Thompson and H. Yersin, *Inorg. Chem.*, 2009, **48**, 1928–1937.
102 Typically, powder samples exhibit strong concentration quenching effects, for example, due to energy transfer to defect sites. However, in Cu(I) compounds typically a geometry distortion occurs on excitation, resulting in the trapping of the excitation on one molecule.[28,29,32] This effect seems to prevent concentration quenching.
103 J. S. Wilson, N. Chawdhury, M. R. A. Al-Mandhary, M. Younus, M. S. Khan, P. R. Raithby, A. Köhler and R. H. Friend, *J. Am. Chem. Soc.*, 2001, **123**, 9412–9417.
104 C. Murawski, K. Leo and M. C. Gather, *Adv. Mater.*, 2013, **25**, 6801–6827.
105 W. L. F. Armarego and D. D. Perrin, *Purification of Laboratory Chemicals*, Elsevier, Burlington, 1996.
106 R. N. Keller, H. D. Wycoff and L. E. Marchi, *Inorg. Synth.*, 1946, **2**, 1–4.
107 G. B. Kauffman, L. Y. Fang, N. Viswanathan and G. Townsend, *Inorg. Synth.*, 1983, **22**, 101–103.
108 M. J. Frisch, G. W. Trucks, H. B. Schlegel, G. E. Scuseria, M. A. Robb, J. R. Cheeseman, G. Scalmani, V. Barone, B. Mennucci, G. A. Petersson, H. Nakatsuji, M. Caricato, X. Li, H. P. Hratchian, A. F. Izmaylov, J. Bloino, G. Zheng, J. L. Sonnenberg, M. Hada, M. Ehara, K. Toyota, R. Fukuda, J. Hasegawa, M. Ishida, T. Nakajima, Y. Honda, O. Kitao, H. Nakai, T. Vreven, J. A. Montgomery Jr., J. E. Peralta, F. Ogliaro, M. Bearpark, J. J. Heyd, E. Brothers, K. N. Kudin, V. N. Staroverov, R. Kobayashi, J. Normand, K. Raghavachari, A. Rendell, J. C. Burant, S. S. Iyengar, J. Tomasi, M. Cossi, N. Rega, J. M. Millam, M. Klene, J. E. Knox, J. B. Cross, V. Bakken, C. Adamo, J. Jaramillo, R. Gomperts, R. E. Stratmann, O. Yazyev, A. J. Austin, R. Cammi, C. Pomelli, J. W. Ochterski, R. L. Martin, K. Morokuma, V. G. Zakrzewski, G. A. Voth, P. Salvador, J. J. Dannenberg, S. Dapprich, A. D. Daniels, Ö. Farkas, J. B. Foresman, J. V. Ortiz, J. Cioslowski and D. J. Fox, *GAUSSIAN 09 (Revision A.02)*, Gaussian, Inc., Wallingford, CT, 2009.
109 Stoe & Cie, Stoe & Cie GmbH, Darmstadt, Germany, 2011.
110 Bruker, Bruker AXS Inc., Madison, Wisconsin, USA, 2012.
111 A. Altomare, M. C. Burla, M. Camalli, G. Cascarano, C. Giacovazzo, A. Guagliardi, A. G. G. Moliterni, G. Polidori and R. Spagna, *J. Appl. Crystallogr.*, 1999, **32**, 115–119.
112 G. Sheldrick, *Acta Crystallogr., Sect. A: Fundam. Crystallogr.*, 2008, **64**, 112–122.
113 A. L. Spek, *Acta Crystallogr., Sect. D: Biol. Crystallogr.*, 2009, **65**, 148–155.
114 L. Farrugia, *J. Appl. Crystallogr.*, 1999, **32**, 837–838.
115 R. H. Blessing, *Acta Crystallogr., Sect. A: Fundam. Crystallogr.*, 1995, **51**, 33–38.
116 N. W. Alcock, in *Cryst. Computing*, ed. F. R. Ahmed, S. R. Hall and C. P. Huber, Munksgaard, Copenhagen, 1970, pp. 271–276.
117 Bruker, Bruker AXS Inc., Madison, Wisconsin, USA, 2012.
118 K. Brandenburg and H. Putz, Crystal Impact GbR, Bonn, Germany, 2012.

